Estonian Journal of Earth Sciences, 2020, **69**, 1, 37–61 https://doi.org/10.3176/earth.2020.03

Middle Ordovician carbonate facies development, conodont biostratigraphy and faunal diversity patterns at the Lynna River, northwestern Russia

Anders Lindskog[a,b], Mats E. Eriksson[a], Jan A. Rasmussen[c], Andrei Dronov[d,e] and Christian M. Ø. Rasmussen[f,g]

[a] Department of Geology, Lund University, Sölvegatan 12, SE-22362 Lund, Sweden; anders.lindskog@geol.lu.se, mats.eriksson@geol.lu.se
[b] Department of Earth, Ocean & Atmospheric Science, Florida State University, 1017 Academic Way, Tallahassee, FL 32306, USA
[c] Fossil and Moclay Museum, Museum Mors, Skarrehagevej 8, Nykøbing Mors, DK-7900, Denmark; jan.rasmussen@museummors.dk
[d] Institute of Geology, Russian Academy of Sciences, Pyzhevsky per. 7, Moscow, 119017, Russia; dronov@ginras.ru
[e] Kazan (Volga Region) Federal University, 18 Kremlevskaya Street, Kazan 420008, Russia
[f] Natural History Museum of Denmark, University of Copenhagen, Øster Voldgade 5–7, 1350 Copenhagen K, Denmark; christian@snm.ku.dk
[g] Section for Geobiology, GLOBE Institute, University of Copenhagen, Øster Voldgade 5–7, 1350 Copenhagen K, Denmark

Received 12 September 2019, accepted 19 December 2019, available online 28 January 2020

Abstract. The Ordovician Period has emerged as a highly dynamic time in Earth history. Comprehensive work on chrono-, chemo- and biostratigraphy has resulted in an overall well-constrained systemic framework, but several local successions around the globe still await detailed analysis in many respects. Herein we perform a high-resolution analysis of abiotic and biotic signals in the Lynna River section, a key locality in northwestern Russia. As this section has been pivotal in documenting the temporal evolution of the Great Ordovician Biodiversification Event on Baltica, the macroscopic and microscopic characteristics of the local succession reveal important paleoenvironmental information that ties into the global development during the Middle Ordovician. The results add particularly to the understanding of the characteristics and large-scale sedimentary 'behavior' of the Baltoscandian paleobasin. Microfacies vary consistently with the macroscopic appearance of the rocks, with intervals characterized by competent limestone being associated with coarser carbonate textures and intervals dominated by marly beds associated with finer textures. Along with carbonate textures, fossil grain assemblages vary in a rhythmic (~cyclic) manner. The local rocks are commonly partly dolomitized, with the proportion of dolomitization increasing up-section. Regional comparisons suggest that the changes in overall macro- and microfacies were strongly related to variations in sea level. New high-resolution conodont biostratigraphic data largely confirm previous regional correlations based on lithostratigraphy and trilobite faunas, and enable more robust correlations worldwide.

Key words: carbonate sedimentology, microfacies, paleoecology, sea level, Great Ordovician Biodiversification Event, St Petersburg region, Baltica.

INTRODUCTION

Ordovician sedimentary rocks record profound changes in the global abiotic and biotic realms. Comprehensive research during the last decades has led to the establishment of detailed chemo- and biostratigraphic schemes through the entire Ordovician (e.g., Bergström et al. 2009, and references therein). Coupled with a longterm historic tradition of deciphering the strata with regard to lithological and paleontological properties, the Ordovician has emerged as one of the most dynamic and eventful periods of the Phanerozoic, comprising prominent and widespread faunal diversifications, isotopic excursions, and ending with the first of the 'Big Five' Phanerozoic mass extinction events (e.g., Webby et al. 2004; Harper et al. 2014). Still, our knowledge about the interconnection and interplay between life and the environment remains incomplete and is in need of detailed assessment of key outcrops. This, together with an overall limited understanding of how ancient epeiric seas behaved, provides incentive for further detailed work.

The East Baltic area hosts numerous excellent outcrops of lower Paleozoic strata and the St Petersburg (temporarily Petrograd, Leningrad) region in Russia has

long held a prominent role in the scientific work concerning the Ordovician System (e.g., Pander 1830; Schmidt 1858, 1881, 1882; Lamansky 1905; Alikhova 1960; Sergeyeva 1962). The regional sedimentary succession has become an important archive for the understanding of the paleontologic and paleoenvironmental development during the Great Ordovician Biodiversification Event (GOBE; e.g., Tolmacheva et al. 1999; Hansen & Harper 2003; Rasmussen et al. 2007, 2009, 2016; Koromyslova 2011; and references therein) and the strata even hold possible clues to events in our solar system (Korochantsev et al. 2009; Lindskog et al. 2012; Heck et al. 2016, 2017). Recent global biodiversity data highlight the lowermost Darriwilian – the very interval covered by the succession at the Lynna River – as pivotal for the biotic development during the GOBE (Rasmussen et al. 2019).

In this study, we document the biotic and sedimentary development in close detail through the exposed succession at the Lynna River, northwestern Russia, and investigate the local conodont fauna. The conodont zonation at the Lynna River has previously only been inferred from studies elsewhere in Baltoscandia, and the establishment herein of the local framework enables more robust regional and global correlations. This in turn enables better assessment of local faunal diversity changes and environmental perturbations that hitherto have been problematic to compare with the global record at a high temporal resolution (Rasmussen et al. 2016; Lindskog et al. 2017). The collective data form the basis for the evaluation of the local depositional environment and connecting its temporal development across biozonal frameworks to coeval changes in the Middle Ordovician paleobasin of Baltoscandia.

GEOLOGIC SETTING

Throughout the Ordovician, large parts of Baltoscandia (which in geologic terms includes westernmost Russia; historically referred to as Ingria) were covered by an epeiric sea, which left behind a laterally extensive, albeit typically thin, blanket of sedimentary rocks. Severely peneplaned land areas resulted in limited terrigenous input to the paleobasin and net sedimentation rates were typically on the order of millimeters per millennia (e.g., Männil 1966; Lindström 1971; Jaanusson 1973; Lindskog et al. 2017). The paleocontinent Baltica was situated in the southern hemisphere and on a move northward (Cocks & Torsvik 2006; Torsvik & Cocks 2017). This continental drift is reflected in the regional geologic development, with the Ordovician succession showing a gradual transition from cold- and cool-water (subpolar–temperate) into warm-water (subtropical–tropical) deposits (see Dronov & Rozhnov 2007). During the Middle Ordovician, Baltica was situated in temperate latitudes.

Cambrian and Ordovician rocks are exposed along the so-called Baltic–Ladoga Klint, a natural escarpment extending some 1200 km from the southern part of the Baltic Sea through the northern coast of Estonia and into western Russia (Fig. 1; e.g., Schmidt 1882). In the St Petersburg region, Ordovician rocks form a topographic high known as the Ordovician Plateau. The regional Ordovician succession is 100–200 m thick and mainly characterized by carbonate rocks. The rock successions record a north-to-south and west-to-east deepening of the shelf (or, carbonate ramp) and, thus, strata tend to thicken towards the east and south whereas they thin out towards the north and west. To the east of St Petersburg, several natural exposures have been cut into the Paleozoic rocks by rivers that drain into Lake Ladoga, offering ample opportunity for quarrying (e.g., Popov 1997; Dronov et al. 2005; Dronov & Mikuláš 2010). The many natural and manmade outcrops in the area have provided an excellent basis for a long tradition of scientific study of the regional rocks. Illustrative accounts of earlier scientific studies can be found in Raymond (1916) and Dronov & Mikuláš (2010).

Just south-southwest of the village of Kolchanovo, *c*. 150 km east of St Petersburg, Middle Ordovician sedimentary rocks crop out along the Lynna River. An excellent exposure has long been known in the valley close to the mouth of the river, where it drains into the larger Syas River (WGS 84 coordinates 60.010833, 32.563611). The local succession is *c*. 10 m thick and mainly characterized by alternation between limestone and variably silty–sandy calcareous mud (henceforth termed 'marl'). It spans the uppermost middle Volkhov through middle Kunda regional stages (e.g., Dronov & Mikuláš 2010), corresponding to the uppermost Dapingian through lowermost middle Darriwilian global stages (Fig. 2). The succession is divided, in stratigraphically ascending order, into the Volkhov, Lynna, Sillaoru and Obukhovo formations. The Volkhov Formation largely hosts beds of the eponymous Volkhov Regional Stage, whereas the overlying formations belong to the Kunda Stage (cf. Mägi 1984; Ivantsov 2003). The succession at the Lynna River is relatively expanded and stratigraphically more complete as compared to most other outcrops along the Baltic–Ladoga Klint (e.g., Lamansky 1905; Männil 1966; Raukas & Teedumäe 1997).

The strata at the Lynna River span a crucial phase of the GOBE (*sensu* Rasmussen et al. 2019), and locally collected faunal diversity, geochemical and paleoenvironmental data have added immensely to the understanding of this global phenomenon in the history

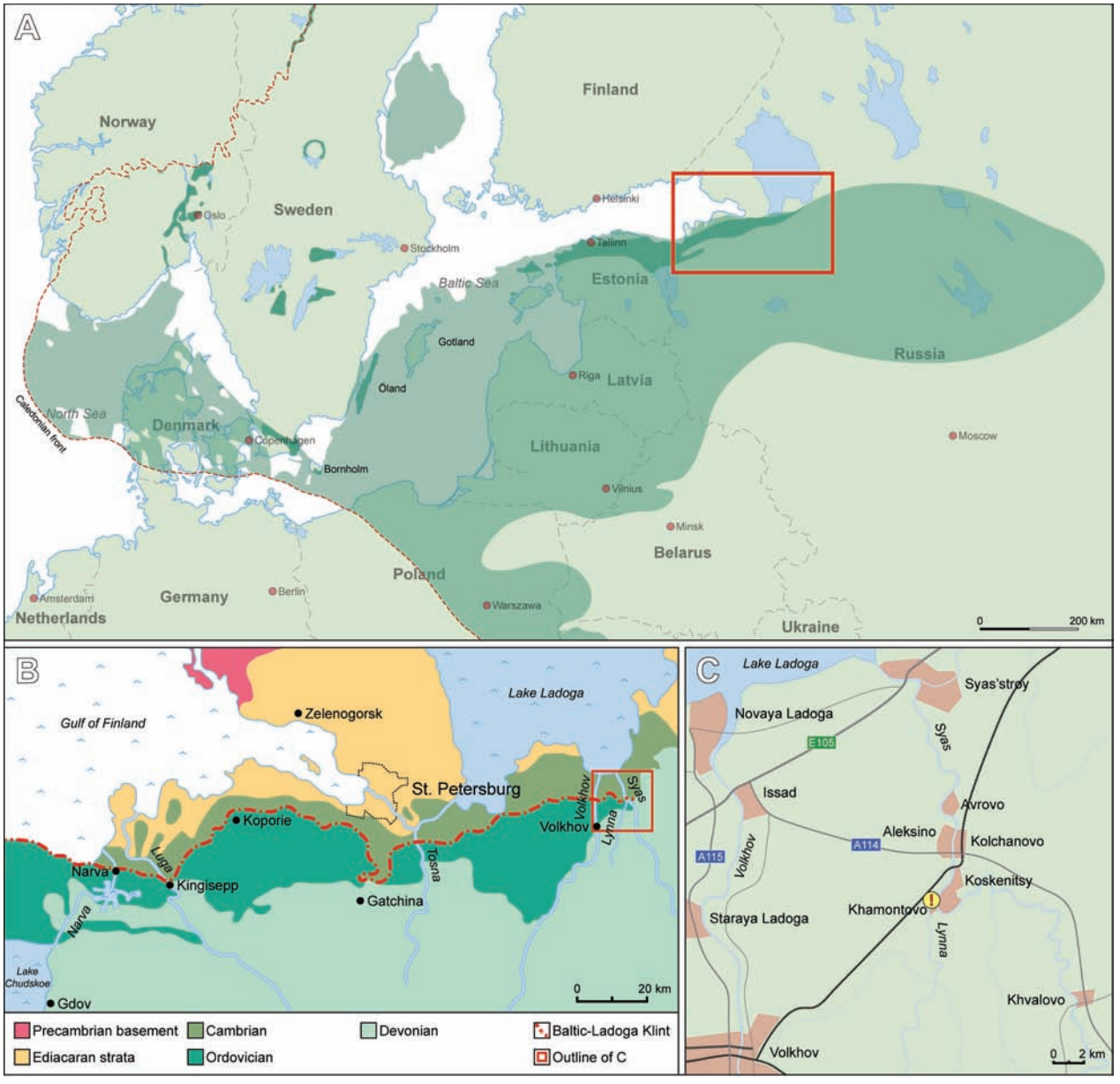

Fig. 1. A, map of the Baltoscandian region, with the approximate distribution of lower Paleozoic strata indicated by green shading; darker shaded areas indicate areas with significant outcrops of Ordovician strata (modified from Lindskog & Eriksson 2017, with additions after Jaanusson 1982a and Lindskog et al. 2018). The red rectangle indicates the outline of the map area in B. **B**, map of the St Petersburg region, with the distribution of rocks indicated (modified from Lindskog et al. 2012). **C**, map of the study locality and its surroundings.

of life on Earth (e.g., Rasmussen et al. 2007, 2009, 2016; Trubovitz & Stigall 2016). As has been shown for coeval strata at various localities in Sweden (e.g., Schmitz et al. 2003), and in South China (Cronholm & Schmitz 2010), beds near the lower–middle Kunda boundary at the Lynna River are enriched in chromite grains of extraterrestrial origin (Korochantsev et al. 2009; Lindskog et al. 2012; Meier et al. 2014). Together with numerous fossil meteorites recorded in Sweden, this abundance of extraterrestrial chromite has been associated with the catastrophic breakup of the L chondrite parent body in the asteroid belt close to this time (see Heck et al. 2016, 2017; Lindskog et al. 2017; and references therein).

MATERIALS AND METHODS

After clearing a composite section, nearly the entire succession at the Lynna River was studied and sampled *in situ*; the basal beds of the local succession were

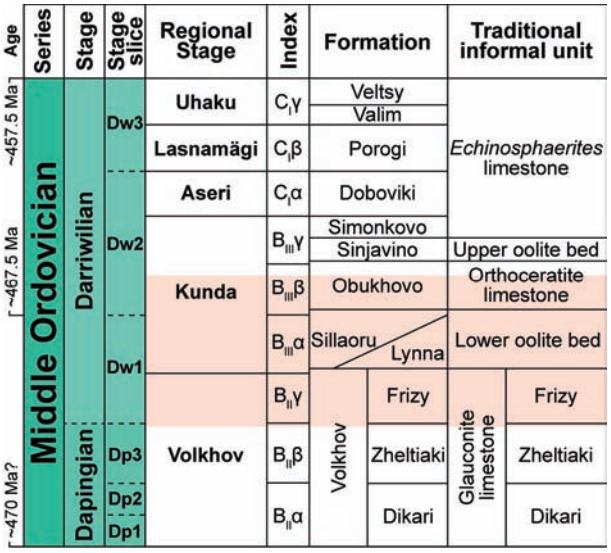

Fig. 2. The Middle Ordovician stratigraphic framework of the St Petersburg area with Baltoscandian and global stratigraphy for comparison (modified from Lindskog et al. 2012, with additions according to Bergström et al. 2009; Lindskog et al. 2017; Normore et al. 2018). The shaded area indicates the approximate stratigraphic range of the outcrop at the Lynna River.

consistently inaccessible due to high water levels (Figs 3, 4). The base of a distinct bed with rusty red and poorly lithified marl, visibly strewn with limonite-stained grains, was used as a reference (0 m) level during measurements (Figs 3D, 4). This level coincides with the boundary between the *Asaphus expansus* and *Asaphus raniceps* trilobite zones, as well as the boundaries between the Lynna and Sillaoru formations (e.g., Ivantsov 2003). Measurements above the reference level are given as positive numbers and those below as negative numbers. A total of 51 bulk rock samples were collected throughout the succession, giving an average sampling resolution of *c*. 20 cm. Sampling was concentrated to relatively competent limestone banks, but a few levels of largely unconsolidated marl were also targeted for comparative studies.

Representative thin sections were produced from all limestone samples for qualitative and quantitative microfacies analyses (see Flügel 2010). The thin sections were analyzed quantitatively following the approach described by Lindskog & Eriksson (2017). In short, the carbonate texture of each thin section was determined by means of point counting using the grain-bulk method (see Dunham 1962). A total of 600 (300 × 2) points were counted per thin section. In order for the data to better reflect the primary characteristics of the rock-forming sediment (i.e. the depositional environment), areas with fabric-destructive recrystallization (see below) were omitted. Fossil grain assemblages within individual samples were characterized by the identification of 600 (300 × 2) grains. Five separate grain categories were distinguished: Brachiopoda, Echinodermata, Ostracoda, Trilobita and Other (including minor, sometimes ambiguous, fossil components). Unidentifiable grains were counted separately, but not included in the visual data presentation herein; typically, 10–20% of the total grain assemblages represent such grains, most of which are small arthropod fragments (Arthropoda indet.) that clearly co-vary in abundance with trilobites and/or ostracods (see also Lindskog & Eriksson 2017; Lindskog et al. 2018). Carbonate textures and fossil grain assemblages vary somewhat between replicate samples (typically *c*. 5% in grain abundance), but the data nonetheless show consistent longer-term patterns and trends; small-amplitude fluctuations in relative abundances should be interpreted with care (see van der Plas & Tobi 1965; Tolmacheva et al. 2001). The data set amassed during quantitative analyses comprises more than 70 000 data points in total.

Twenty-two kilogram-sized samples were treated with buffered acetic acid for the retrieval of microfossils, according to standard procedures (e.g., Jeppsson et al. 1999). After sieving the acid-insoluble residues, conodont elements were electrostatically handpicked from the >63 μm high-density fractions (light-density materials were kept, but not studied herein). The resulting collections were studied with focus on biostratigraphically and paleoenvironmentally important taxa, in order to determine the biostratigraphic framework at the Lynna River. Photographs of conodont elements were produced with an Olympus SC30 digital camera attached to an Olympus SZX16 stereo microscope, using image stacking techniques via the software cellSens.

All sample materials are stored at the Department of Geology, Lund University, Sweden. Figured conodonts belong to the type collection at the same department and have repository numbers LO (for Lund Original) followed by five digits and t for 'type'.

RESULTS

Sedimentary and biotic development through the Lynna River succession

Field and thin-section observations are summarized in Fig. 4, together with a compilation of previously published geochemically, paleontologically and sedimentologically informative data.

At the outcrop scale, the exposed succession is characterized by grayish-beige colored, in places distinctly red-mottled, rocks showing alternation between

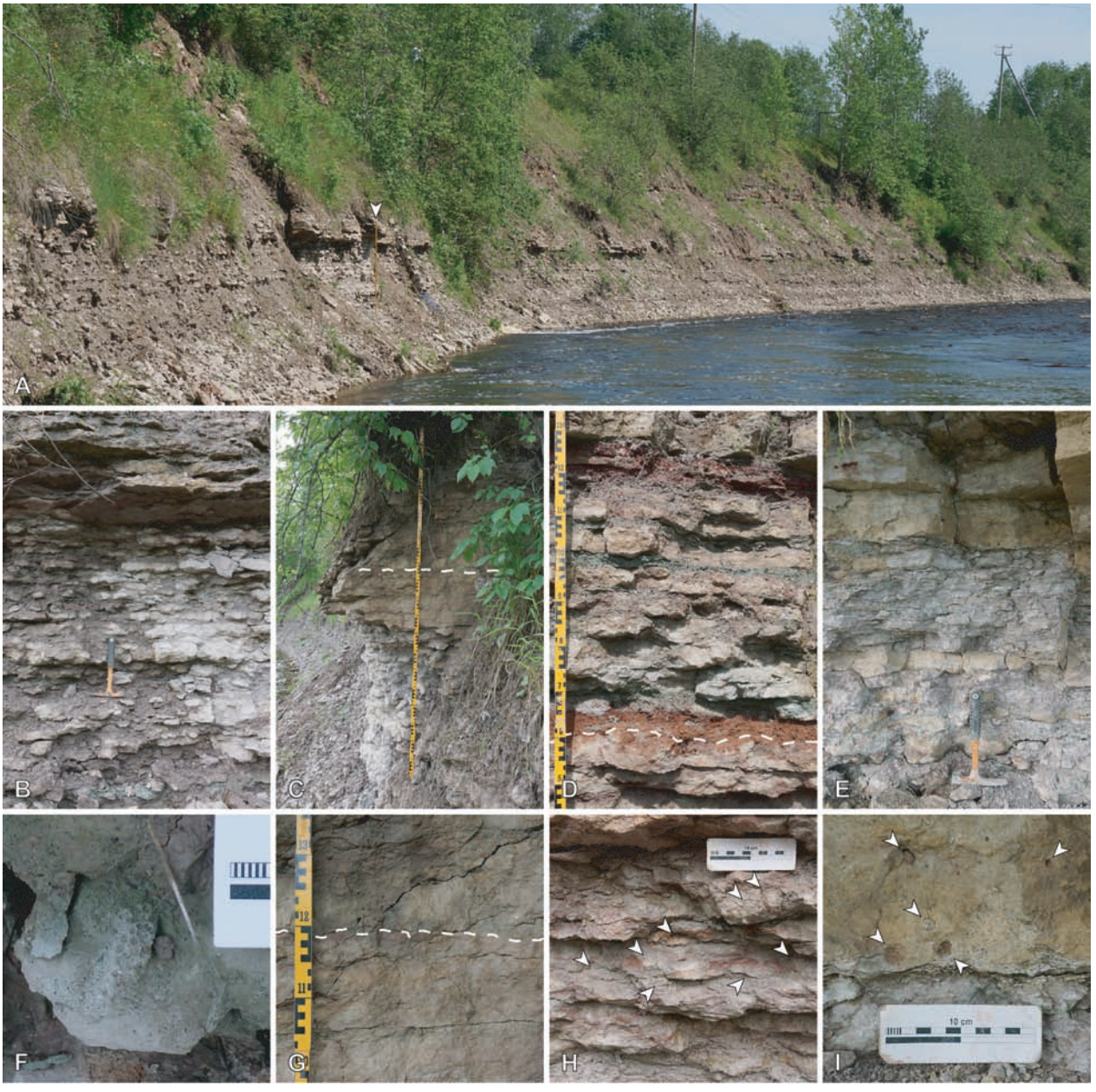

Fig. 3. Field photographs. **A**, the outcrop along the Lynna River, view to the north-northwest. Two-meter measuring stick (white arrow) for scale, resting against the Volkhov–Kunda boundary beds. **B**, the exposed Volkhov Formation is characterized by alternation between limestone beds (typically discontinuous, lens-like) and soft marl. **C**, the beds surrounding the Volkhov–Kunda boundary (stippled line) weather out distinctly, as they comprise relatively dense limestone. **D**, the Sillaoru Formation (basal *A. raniceps* Zone) is characterized by a succession of distinct, variably colored marl beds. The stippled line indicates the Lynna Formation–Sillaoru Formation boundary (*A. expansus–A. raniceps* boundary). **E**, the uppermost part of the succession (Obukhovo Formation) at the Lynna River is characterized by a change from limestone–marl alternation into dense, pale dolomitic limestone (traditionally referred to as the 'White bed'). **F**, a laterally widely traceable surface in the upper Volkhov containing abundant *Trypanites* borings. **G**, close-up of the Volkhov–Kunda boundary beds; the stippled line at the boundary (*A. lepidurus–A. expansus* boundary). **H**, close-up of the uppermost beds of the Lynna Formation (uppermost *A. expansus* Zone). Trilobites (arrows) occur abundantly in association with numerous hematite-stained discontinuity surfaces (~hardgrounds). Articulated fossils are relatively common. **I**, close-up of the basal 'White bed', close to the top of the succession at the Lynna River. This bed is characterized by numerous round weathering cavities, some of which contain argillaceous matter (arrows).

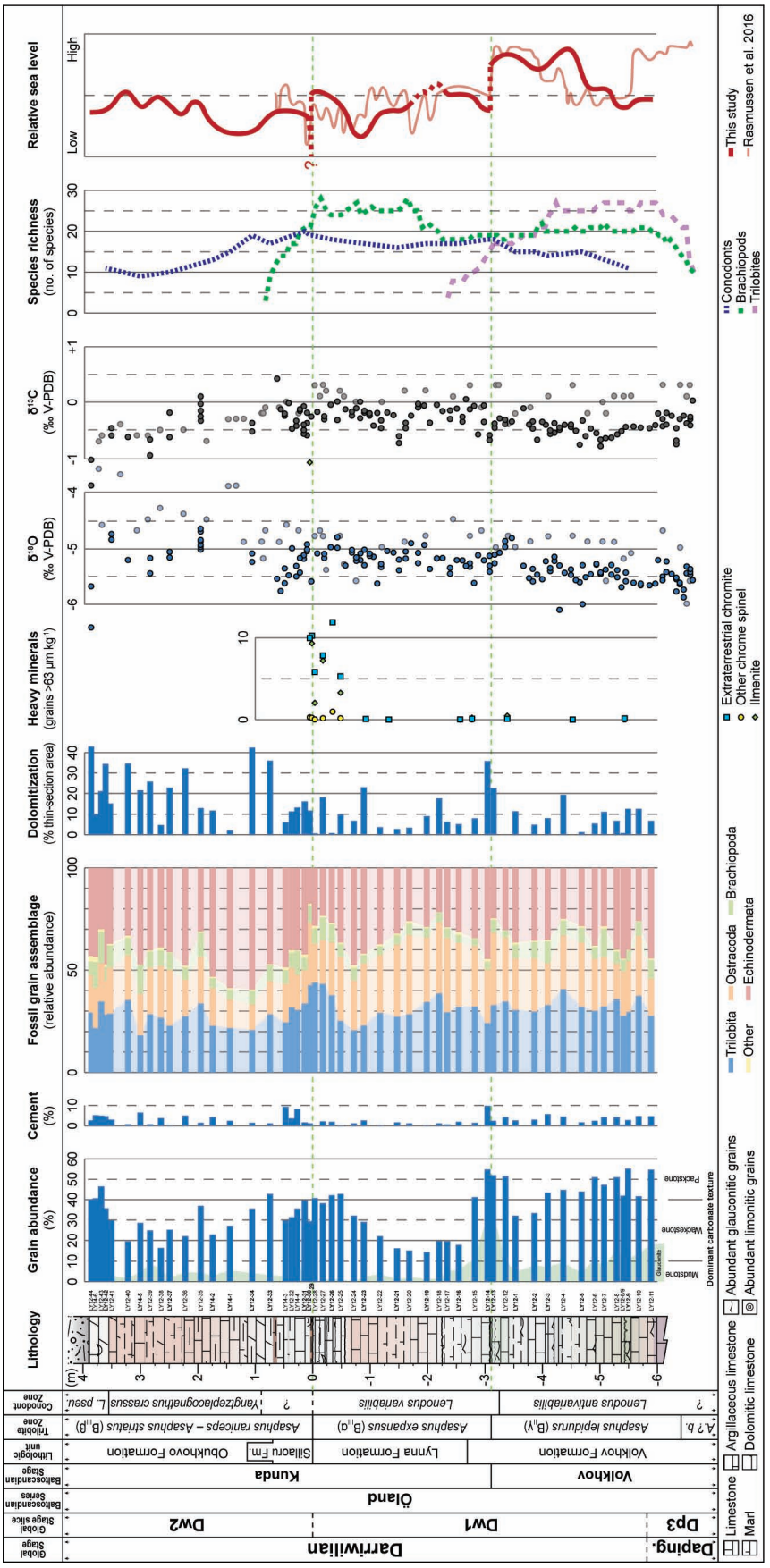

Fig. 4. Sedimentary profile and stratigraphic framework of the outcrop at the Lynna River, together with sedimentologic and chemostratigraphic data, and interpretations of relative sea level. Color variations in the lithologic column are slightly enhanced to emphasize subtle changes through the succession. Sample names in bold denote levels searched for conodonts. Lithostratigraphy and trilobite zonation after Ivantsov (2003); heavy mineral data modified from Lindskog et al. (2012) and Heck et al. (2016, 2017); carbon ($\delta^{13}C$) and oxygen ($\delta^{18}O$) isotope data modified from Zaitsev & Pokrovsky (2014; lighter shaded symbols, based on bulk carbonate samples) and Rasmussen et al. (2016; darker shaded symbols, based on brachiopod shells); brachiopod species richness data from Hansen & Harper (2003) and Rasmussen & Harper (2008); trilobite species richness data from Hansen & Nielsen (2003). *Abbreviations*: Daping., Dapingian; *A.? b.*, *Asaphus? broeggeri*; *L. pseu.*, *Lenodus pseudoplanus*.

relatively competent limestone and easily weathering marl (i.e. poorly lithified calcareous mud with variable amounts of silt–sand-sized particles). A repetitive pattern of intervals dominated by such limestone–marl alternation and intervals with dense limestone beds separated by thin shale-like horizons is apparent throughout the local sedimentary succession (Figs 3A, 4). The local fossil macrofauna is typically dominated by brachiopods and trilobites, both of which commonly occur articulated. Although articulated echinoderms are rare, such debris (mainly from pelmatozoans) is abundant in places, with the enigmatic *Bolboporites* (see Pander 1830; Rozhnov & Kushlina 1994) forming a characteristic component in the Volkhov beds. Trilobites are especially numerous in the upper Volkhov beds and in the Kunda *A. expansus–A. raniceps* boundary interval. Cephalopods occur throughout, but are most numerous in the basal Kunda and the uppermost part of the succession. Several types of ichnofossils occur throughout the succession and include both soft- and hard-bottom forms of variable size. Among these, *Thalassinoides*- and *Balanoglossites*-like burrows/borings, *Arenicolites*, *Palaeophycus* and *Planolites* are the most common, together with occasionally dense populations of *Arachnostega*, *Bergaueria*, *Chondrites* and *Trypanites* (see Dronov & Mikuláš 2010; Knaust & Dronov 2013; Toom et al. 2019).

At the microscopic scale, the local strata are mainly characterized by wackestone and packstone textures (Figs 4, 5). Cement typically occurs in areas with grainstone, in borings and burrows left unfilled by finer sediment and in sheltered rock portions (e.g., within and under grains). Fossil grain assemblages mainly consist of variably abraded fragments of trilobites, ostracods, echinoderms and brachiopods. Other fossil groups are poorly represented, but include mollusks (mainly gastropods and cephalopods), bryozoans, sponges (spicules), conodonts, agglutinating foraminifera and problematica. Bioturbation is typically extensive. Many beds are strewn with cryptocrystalline hematite 'dust' that gives the rock a pinkish–reddish hue. Dissolution seams filled with fine-grained siliciclastic material occur, and abundantly so in marly beds. Apart from glauconite, siliciclastic content in the sand-sized fraction is otherwise sparse, with well-rounded quartz being most common (such grains are relatively abundant in the uppermost Lynna and lower Sillaoru formations). Dolomite occurs throughout the succession and nearly every thin section is affected by dolomitization to some extent (Fig. 5). Dolomite crystals have mainly developed in the matrix, commonly within bioturbation structures, but also in skeletal grains (especially thin-shelled taxa) and originally calcitic cement. The crystals are mainly subhedral to euhedral in shape, with the longest axes from a few micrometers to several hundreds of micrometers, and form planar textures (see Sibley & Gregg 1987). There is a distinct increase in the prevalence of dolomitization and related coarse-calcite recrystallization upward through the stratigraphy. Typically, *c*. 10% of the sample area in thin sections from the Volkhov beds is thoroughly affected by dolomitization (and related other recrystallization), but it increases to *c*. 30–40% in the uppermost (middle Kunda) beds (Fig. 4). Dolomitization broadly follows carbonate texture and argillaceous samples are typically more affected. Dolomitization is clearly associated with the destruction and obscuring of original fabrics, and grain loss (or, rather 'assimilation' due to recrystallization) is commonly extensive. Typically, the apparent grain abundance in strongly recrystallized areas of thin sections is about one-third to half of that of surrounding unaffected rock. Some skeletal grains are partly recrystallized into dolomite even in areas otherwise unaffected by dolomitization (Fig. 5I).

The Volkhov Formation is clearly distinct from the overlying formations due to its high proportion of glauconite grains (Fig. 3B). For obvious reasons, this stratigraphic interval is commonly referred to as the 'Glauconite limestone' in older literature (e.g., Schmidt 1858, 1881, 1882; Lamansky 1905). Packstone and wackestone textures dominate, with patches of grainstone occurring mainly in bioturbation structures and as 'lags' on bedding surfaces (Figs 4, 5I). Glauconite occurs both as matrix-staining impregnation and discrete silt- to sand-sized grains, which are typically sub-rounded to rounded (*sensu* Powers 1953) and commonly show clear signs of reworking (Fig. 5A, K, M). A particularly distinct green-colored bed occurs in the lowermost part of the succession (LY12-8/9, *c*. –5.5 m). In places, the upper surface of this bed is densely populated by *Trypanites* borings (Fig. 3F). This '*Trypanites* bed' is laterally traceable through the entire exposure at the Lynna River and forms a good local and even regional marker level. It can be recognized in the Putilovo quarry, *c*. 70 km to the west, and belongs to the 'Middle unit of intercalation' of the Frizy Member ($B_{II}\gamma$; Dronov & Fedorov 1995). Some beds are rich in fossils, many of which are very well preserved and articulated. Fossil grain assemblages in the Volkhov Formation are variably dominated by arthropods and echinoderms, the relation (in terms of relative abundance) of which seems to vary rhythmically. Ostracods increase in number upward through the stratigraphy, whereas echinoderms decrease slightly. A trend of increasing thickness and lateral continuity of limestone beds is seen in the uppermost Volkhov succession, and the Volkhov–Kunda transition is marked by a *c*. 1-m-thick dense limestone interval that lacks notable marl intercalations (Khamontovo Member of Ivantsov & Melnikova 1998; see also Iskyul 2004). This interval is distinct in the outcrop, as it is relatively resistant to weathering (Fig. 3C).

The limestone beds are characterized by glauconite-rich grayish-beige packstone and grainstone. Individual beds are separated by rugged hematite-stained discontinuity surfaces and the Volkhov–Kunda boundary is marked by a relatively distinct such surface that is overlain by a glauconite 'lag' (Figs 3G, 5B, N). Numerous grains have amassed within topographic lows in the boundary-forming discontinuity surface. Overall, glauconite concentrations

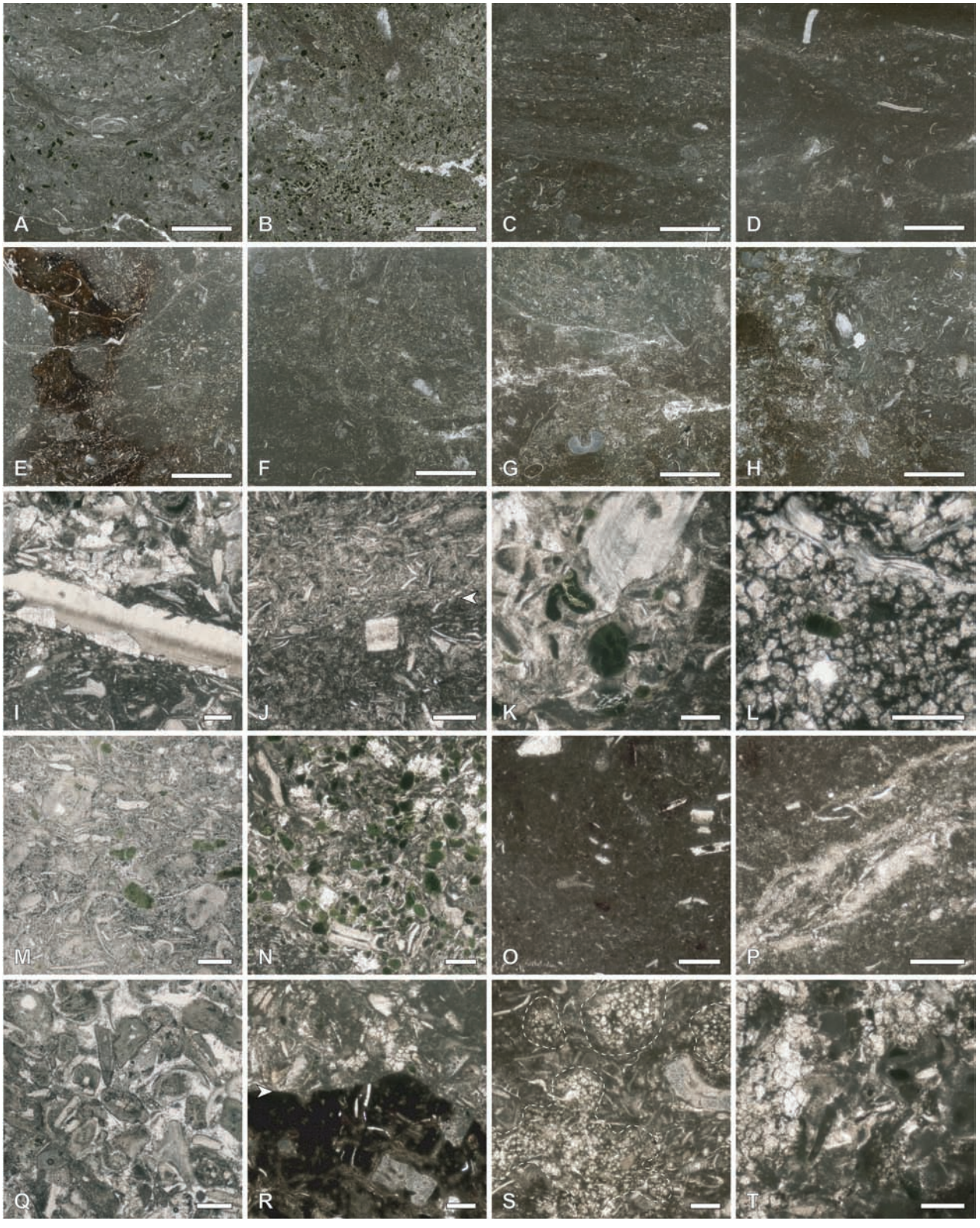

wane slowly through the Volkhov Formation, but a temporary increase embraces the Volkhov–Kunda boundary (Fig. 4).

The basal Kunda beds consist of packstone and grainstone speckled with glauconite grains, but the amount of glauconite quickly decreases up-section (Figs 4, 5C, D). Echinoderms reach a temporary abundance peak among fossil grain components. A gradual change back into limestone–marl alternation is noticeable in the Lynna Formation and the limestone becomes distinctly argillaceous, relatively soft and easily weathered. This change in lithology is associated with a distinct fining of carbonate textures and a subtle change of color into pinkish and reddish hues speckled with greenish reduction spots. Some beds in the middle Lynna Formation show lamination-like internal bedding (Fig. 5C). Dolomitization is occasionally significant. Some horizons contain numerous cephalopod conchs. In grain assemblages, echinoderms rapidly give way to ostracods and the latter reach an abundance acme that spans most of the lower Kunda. Limestone beds thicken and become more laterally continuous again in the uppermost Lynna Formation (the upper *A. expansus* Zone) and the strata return to a grayish-beige color. These beds are characterized by coarse carbonate textures (packstone–grainstone) and numerous rugged and gently undulating hematitic discontinuity surfaces. Many skeletal grains are heavily fragmented, visibly eroded and stained by iron-rich minerals, likely as a result of reworking from older beds and/or unusually long exposure at the seafloor. Brachiopods are common in the macrofossil assemblages and some beds are exceptionally rich in trilobites; many specimens are articulated and exceptionally well preserved, revealing also fine details of the carapace (Fig. 3H). Echinoderms once again dominate the fossil grain assemblages, but are outnumbered by trilobite grains upward. Brachiopods slowly but steadily increase in relative abundance.

The boundary between the Lynna and Sillaoru formations (*A. expansus–A. raniceps* boundary) is marked by a distinct change in lithology, from dense limestone to poorly lithified rusty red marl strewn with limonitic grains (Fig. 3D). The top surface of the uppermost bed of the Lynna Formation contains numerous cavities (corroded burrows/borings?) filled with rusty red sediment stemming from the strata above (Fig. 5E). The bright color and distinct properties of the basal Sillaoru bed makes it an excellent reference level in the local stratigraphy.

The thin Sillaoru Formation (Lower oolite bed in older terminology; Dronov & Mikuláš 2010) is characterized here by a succession of poorly lithified and variably colored marl beds that intercalate with argillaceous wackestone and packstone (Figs 3D, 4). The marly beds contain abundant fragmentary skeletal material and silt- to sand-sized dolomite crystals (see also Tolmacheva et al. 2001, 2003). The overlying Obukhovo Formation marks yet another return to limestone–marl alternation and finer carbonate textures, wherein reddish and greenish marl intercalates with vaguely yellowish argillaceous and dolomitic limestone (Fig. 3E). Echinoderms and brachiopods steadily increase in the fossil grain assemblages upward through the succession, while arthropods decrease in relative abundance. Echinoderms reach a distinct abundance maximum in the basal Obukhovo Formation. Cephalopod conchs become quite common, but many are poorly preserved due to significant diagenetic dissolution of original shell components and distortion from compaction. A slight increase in the amount of glauconitic grains is seen, although these grains typically differ from those of underlying beds in that they mainly constitute shell fillings rather than discrete glauconitic sand grains. Spherical marcasite concretions, in places reaching centimeter-size, with radial internal crystal structures occur frequently (Fig. 3I). The uppermost part of the exposed succession at the Lynna River is characterized

Fig. 5. Thin-section micrographs. Scale bars in A–H 5 mm (transmitted light; images to the same scale for direct comparison), I–P 500 μm (plane-polarized light). **A**, glauconite-speckled wackestone in the basal part of the exposed succession at the Lynna River (Volkhov Formation; sample LY12-11). Note the distinct U-shaped burrow (~*Arenicolites* isp.; e.g., Dronov & Mikuláš 2010) in the center. **B**, glauconitic wackestone–packstone overlying the Volkhov–Kunda boundary (LY12-14). **C**, wackestone in the lower Lynna Formation, showing lamination-like structure (LY12-15). Note the abundance of ostracods (thin vaulted valves). **D**, mudstone–wackestone in the middle Lynna Formation (LY12-21). Bioturbation patterns are associated with dolomitization of the matrix. **E**, cavities in the uppermost (wackestone) bed of the Lynna Formation, filled with reddish material from overlying marl (LY12-28). Note the presence of limonitic grains. **F**, wackestone in the Sillaoru Formation (LY12-31). Small dolomite crystals are scattered throughout. **G**, dolomitic wackestone in the Obukhovo Formation (LY12-37). **H**, wackestone–packstone in the uppermost part of the succession at the Lynna River ('White bed', Obukhovo Formation; LY12-44). The left part of the image shows severe fabric-destructive dolomitization. **I**, a trilobite sclerite partly substituted with dolomite. Note bioerosion in grains (LY12-3). **J**, indistinct wackestone bedding surface (white arrow) overlain by dense packstone (LY12-5). **K**, various forms of glauconite grains. Note apparent 'hollowing-out' (bioerosion?) of grain near center (LY12-6). **L**, close-up of heavily dolomitized marly limestone (LY12-7). **M**, glauconitic echinoderm-rich packstone (LY12-9). **N**, glauconite-rich wacke-packstone in the Volkhov–Kunda boundary interval. Note the general rounding of glauconite grains (LY12-13). **O**, calcareous mudstone (LY12-19). **P**, patches and streaks of finely crystalline calcite and dolomite tracing a burrow (LY12-19). **Q**, echinoderm-rich grainstone (LY12-24). **R**, eroded phosphate-impregnated hardground overlain by slightly dolomitic wackestone (LY12-31). **S**, partly dolomitized wacke-packstone. Note destruction of original fabrics and texture in the most heavily dolomitized portions (outlined, originally burrows/borings?; LY12-32). **T**, heavily dolomitized echinoderm-rich packstone (LY12-36).

by an interval of dense limestone beds that weather out distinctly as they are quite resistant. These beds, which are jointly referred to as the 'White bed' (Lamansky 1905), are pale and whitish-beige in color, sometimes with a tinge of purple. Numerous millimeter- to centimeter-sized rounded/spherical cavities from the weathering of marcasite concretions occur, which in places are filled with a brownish flaky and poorly lithified argillaceous matter. The uppermost beds abound with large cephalopod conchs, most of which occur in a single horizon close to the top of the exposed succession. Recrystallization is extensive in the 'White bed' and large areas in thin sections consist of dense patches of grainy dolomite (Fig. 5H).

Conodont succession and zonation

Results from the conodont studies are presented in Fig. 6 and elements of key taxa are shown in Fig. 7. Conodont elements occur in large numbers (typically thousands of elements per kilogram of rock) throughout the succession at the Lynna River and most specimens are well to excellently preserved. Color alteration index (CAI) values of ~1 suggest negligible (<50–80°) heating of the rocks (Epstein et al. 1977). The conodont fauna is dominated by *Baltoniodus* and *Drepanoistodus* associated with common occurrences of *Microzarkodina*, *Scalpellodus* and *Semiacontiodus.* The upper Volkhov and Kunda conodont zonation established for the inner and middle parts of the Baltoscandian platform by Zhang (1998b) and Löfgren (2000a, 2003, 2004) has mainly been followed in the present study. The *Lenodus antivariabilis*-bearing interval is regarded as the *L. antivariabilis* Zone (see Bagnoli & Stouge 1997; Zhang 1998a, 1998b), rather than a subzone of the *Baltoniodus norrlandicus* Zone as preferred by Löfgren (2000a, 2000b).

The* Lenodus antivariabilis *Zone

The major part of the Volkhov Formation belongs to the *Lenodus antivariabilis* Zone (Fig. 6; e.g., Löfgren 2000b). Although confidently identified *Lenodus antivariabilis* specimens were observed only in the uppermost meter of the Volkhov strata, it is probable that also the underlying studied part of the Volkhov Formation belongs to the *L. antivariabilis* Zone. This correlation is especially based on the co-occurrence of *B. norrlandicus* (Fig. 7A, B), *Microzarkodina bella*, *Microzarkodina parva* and *Scalpellodus gracilis* (e.g., Löfgren 2000b), together with *Parapanderodus* sp. and *Semiacontiodus davidi* in the basal interval.

The* Lenodus variabilis *Zone

The *L. antivariabilis* Zone is succeeded upward by the *Lenodus variabilis* Zone close to the Volkhov–Kunda boundary, as indicated by the appearance of the nominal species (Fig. 6). The *L. variabilis* Zone covers the very top of the Volkhov Formation and all of the superjacent Lynna Formation. The base of the zone is indicated by the first occurrence of *L. variabilis* (Fig. 7G–J) together with *Semiacontiodus cornuformis* (*sensu lato*, characterized by a central, posterior, longitudinal groove; Fig. 7E) and *Parapanderodus quietus*. *Drepanoistodus stougei* (Fig. 7C, D) occurs throughout the *L. variabilis* Zone. *Microzarkodina hagetiana* appears for the first time approximately one meter below the top of the zone.

Uncertain interval

The Sillaoru and basal Obukhovo formations are of unclear zonal belonging. This *c*. one-meter-thick interval contains *Lenodus variabilis* together with rare specimens of a species that contains a short posteriolateral process diverging from the middle part of the posterior process in the sinistral Pa element. This development is typical in Pa elements of *Yangtzeplacognathus crassus*, but because the angle between the two processes is wider here than in *Y. crassus sensu stricto*, we have assigned it as *Yangtzeplacognathus*? aff. *crassus* (Fig. 7L; e.g., Zhang 1997, 1998a; Mellgren 2011). Other important species that occur for the first time in this 'uncertain interval' are *Semiacontiodus cornuformis sensu stricto* (Fig. 7F), *Baltoniodus medius* (Fig. 7Q–T) and *Lenodus*? n. sp. A (see Mellgren & Eriksson 2010, fig. 8AK), while *Drepanoistodus balticus* (also frequently named *Drepanoistodus venustus* or *Venoistodus balticus*; Fig. 7K) appears for the first time immediately below the base of the interval. A single specimen of *Microzarkodina* with two denticles in front of the cusp (*M.* aff. *ozarkodella*) was observed in the lower part of the interval, but it is by far outnumbered by specimens with only one anterior denticle. In approximately the same level, large, relatively short-based, geniculate elements regarded as a variety of *Drepanoistodus basiovalis* were observed (Fig. 7V–W).

The* Yangtzeplacognathus crassus *Zone

Confidently identified *Yangtzeplacognathus crassus* specimens (Fig. 7M–P) first appear in the basal Obukhovo Formation (Fig. 6). Specimens of this species, especially the Pa elements, are typically very small and/or poorly preserved in the Lynna River section, but contain diagnostic characteristics that separate them from other platform taxa (Zhang 1997; Löfgren & Zhang 2003). The species *Y. crassus* has been referred to the genus *Lenodus* by some authors (e.g., Rasmussen et al. 2013; Mestre & Heredia 2017). Originally, Zhang (1998a, 1998b) defined the *Yangtzeplacognathus crassus* Zone as a taxon-range

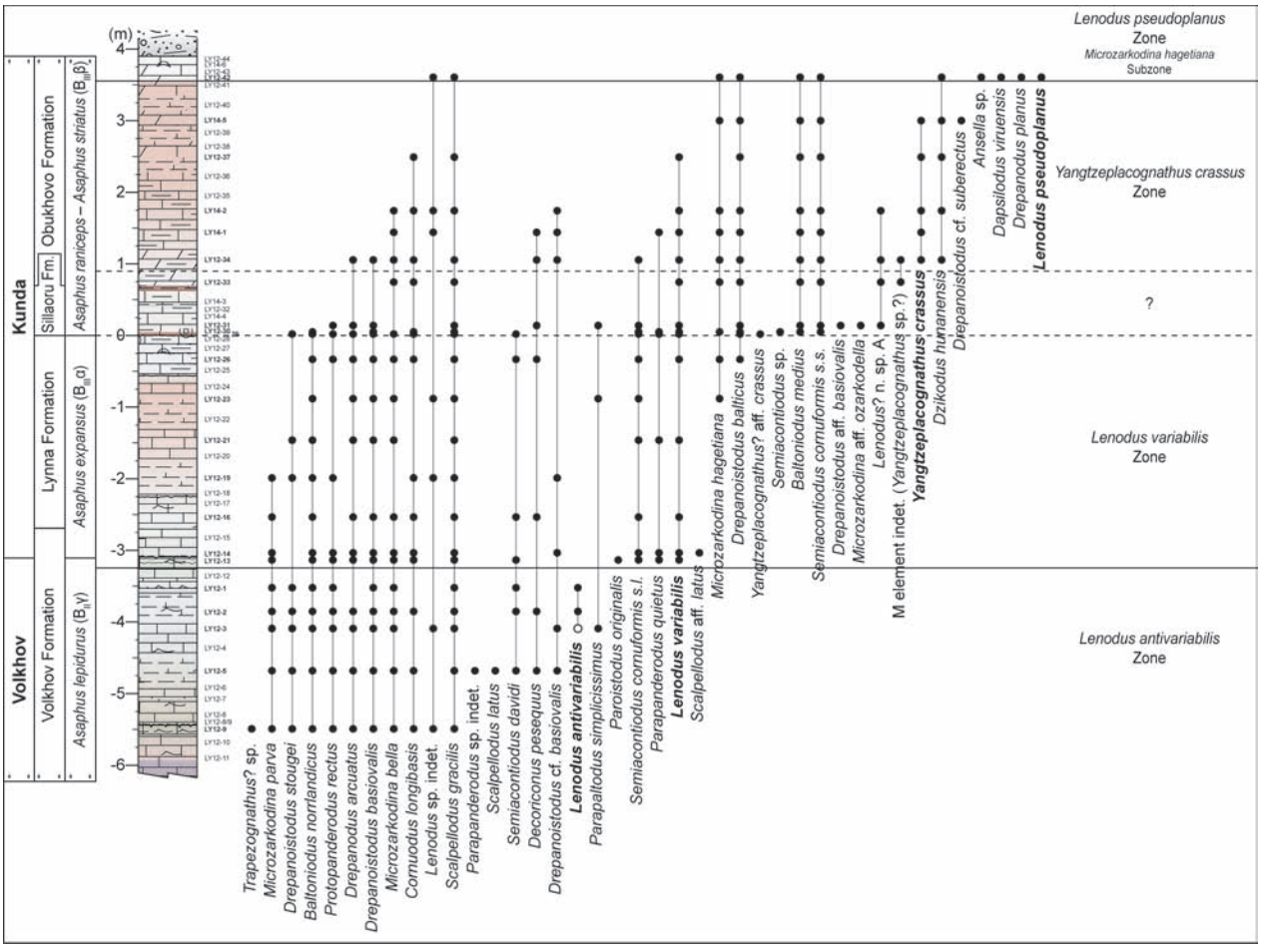

Fig. 6. Lithologic profile together with ranges of conodont taxa and biozonation. For legend, see Fig. 4.

zone based on the occurrence of the nominal species. It may be argued, however, that the first occurrence of *Lenodus pseudoplanus* is a more reliable zonal boundary indicator than the last occurrence of *Y. crassus* (see below). As such, the base of the superjacent *L. pseudoplanus* Zone is here placed at the first occurrence of the nominal species.

The Lenodus pseudoplanus *Zone*

The uppermost *c*. 0.5 m of the studied succession belongs to the *Lenodus pseudoplanus* Zone (commonly referred to as the *Eoplacognathus pseudoplanus* Zone). See Stouge & Bagnoli (1990), Löfgren & Zhang (2003) and Mellgren (2011) for discussions on the nominal species. The lower boundary of the zone is situated *c*. 2.8 m above the base of the Obukhovo Formation (Fig. 6). In addition to *L. pseudoplanus* (Fig. 7X–AA), *Ansella* sp. (Fig. 7AB) and *Dapsilodus viruensis* (Fig. 7AC) occur for the first time in this zone, where *Baltoniodus medius*, *Microzarkodina hagetiana* and *Drepanoistodus balticus* (Fig. 7K) are common. Altogether, this indicates that the uppermost part of the Lynna section belongs to the *M. hagetiana* Subzone of the *L. pseudoplanus* Zone (e.g., Löfgren 2004).

DISCUSSION

The Middle Ordovician carbonate rocks in the St Petersburg region have been interpreted as tempestites formed in a storm-dominated shallow-marine ramp environment (e.g., Dronov 1997a, 1998; Dronov et al. 2002; Hansen & Nielsen 2003; Dronov & Mikuláš 2010). As such, individual beds may have formed rapidly although net sedimentation rates were low. At the Lynna River, tempestite characteristics are indicated by brachiopod biofacies data that exhibit mixing of shallow and deeper water faunas (Rasmussen et al. 2009). The collective data herein support a tempestite-like mode of formation for the local strata, but also show that the depositional environment varied more

than is immediately apparent to the naked eye. The strata at the Lynna River appear to record fluctuations in the paleoenvironment through changes in both macro- and microfacies. As was documented and discussed in detail by Lindskog & Eriksson (2017; see further references therein), the microfacies characteristics of coeval strata of the Middle Ordovician 'orthoceratite limestone' in southern Sweden appear to have varied with relative sea level. In a fashion similar to siliciclastic sediments, the carbonate textures of these cool-water carbonates varied inversely with sea level, such that a relatively low sea level resulted in coarser textures and vice versa for a higher sea level. Moreover, the biota reacted to changes through migration and reorganization, as is recorded by the fossil grain assemblages through changes in the relative abundance of different faunal groups. The same is also seen among trace fossils, as has been well documented especially for the Volkhov interval (Dronov et al. 2002; Knaust et al. 2012). A similar

connection between sea level, carbonate microfacies and the fossil biota (including macrofossil assemblages; see Rasmussen et al. 2009) is suggested at the Lynna River (Fig. 4) and the perceived changes in sea level largely follow those documented by, for example, Dronov (1997b, 1999), Dronov et al. (1998, 2001), Tolmacheva et al. (1999), Dronov & Holmer (2002), Rasmussen et al. (2009, 2016), Knaust et al. (2012), Lindskog & Eriksson (2017) and Lindskog et al. (2018), although further detailed studies of East Baltic localities are needed in order to analyze possible variations in sedimentary 'behavior' across greater parts of the paleobasin. Some notable differences between the Lynna River and hitherto studied Swedish sections are that some of the coarsest carbonate textures at the first locality appear to correspond to relatively deep water (possibly due to related condensation; see below) and the most argillaceous limestone strata are associated with relatively shallow water. These observations hint at complex sedimentary dynamics at the regional scale, and further detailed sedimentologic studies may help solve long-standing contradictions between interpretations concerning sea level history (cf. Nielsen 2004, 2011; Dronov et al. 2011). Lateral, vertical and within-sample variations are more pronounced at the Lynna River than in coeval beds in Sweden, and glauconite concentrations in the Volkhov beds offset carbonate textures, as does abundant fine-grained siliciclastic matter in the Kunda interval. Still, the main stratigraphic patterns, trends and 'event' levels in the microfacies data are unmistakable, and the similarities in microfacies development between geographically distant localities are remarkable. It is unclear to what extent (if any) the limestone–marl alternation that characterizes much of the succession at the Lynna River is of primary origin (see, e.g., Westphal et al. 2008, 2010); any possible connection between the apparently repetitive changes in macroscopic bedding and high-frequency paleoenvironmental changes (such as due to Milankovitch cyclicity) require further detailed analyses of petrographic characteristics and careful consideration of unstable sedimentation (see below).

Overall, there is a distinct difference in both litho- and biofacies between Russia and Estonia, and areas located further west- and southward, indicating significant variations in the depositional environment at the regional scale (e.g., Männil 1966; Jaanusson 1976, 1995). This is reflected in microfacies characteristics, but more studies are needed in order to refine the large-scale picture. Compared to data from south-central Sweden (e.g., Olgun 1987; Lindskog & Eriksson 2017; Lindskog et al. 2018), it is obvious that western Russia represents a more consistently energy-rich depositional environment that was closer to mainland weathering sources during the Ordovician. The carbonate ramp of the St Petersburg region faced a large embayment within the Baltoscandian paleobasin, the so-called Moscow Basin, which caught much of the weathering products from the surrounding land areas (e.g., Jaanusson 1973; Põlma 1982). This entailed distinctly argillaceous carbonates compared to those in much of the western parts of Baltoscandia, which were deposited in more distal (although not necessarily deeper-water) settings oceanward (see Kröger & Rasmussen 2014; Lindskog & Eriksson 2017; Rasmussen & Stouge 2018).

Paleoenvironmental development

A relative sea level curve based on the collective macro- and microfacies data is presented in Fig. 4. Overall, the curve agrees well with that produced by Rasmussen et al.

Fig. 7. Images of selected key conodont taxa, reflected light. Scale bar 200 μm (all elements to the same scale and with identical exposure time). **A**, *Baltoniodus norrlandicus* (Löfgren), Sc element (LY12-1, LO 12443t). **B**, *Baltoniodus norrlandicus* (Löfgren), Sb (LY12-2, LO 12444t). **C**, *Drepanoistodus stougei* Rasmussen (LY12-1, LO 12445t). **D**, *Drepanoistodus stougei* Rasmussen (LY12-29, LO 12446t). **E**, *Semiacontiodus cornuformis sensu lato* (Sergeeva) (LY12-29, LO 12447t). **F**, *Semiacontiodus cornuformis sensu stricto* (Sergeeva) (LY14-5, LO 12448t). **G**, *Lenodus variabilis* (Sergeeva), dextral Pa (LY12-33, LO 12449t). **H**, *Lenodus variabilis* (Sergeeva), M (LY12-13, LO 12450t). *Lenodus variabilis*-like M elements with a rounded carina instead of a sharp costa on the inner side of the base (occurring in samples LY12-1 and LY12-2) have been referred to *Lenodus antivariabilis* instead of *L. variabilis* (*sensu* Löfgren & Zhang 2003). **I**, *Lenodus variabilis* (Sergeeva), M (LY12-26, LO 12451t). **J**, *Lenodus variabilis* (Sergeeva), sinistral Pa (LY12-33, LO 12452t). **K**, *Drepanoistodus balticus* (Löfgren) (LY12-33, LO 12453t). **L**, *Yangtzeplacognathus* aff. *crassus* (Chen & Zhang), sinistral Pa (LY12-29, LO 12454t). The sinistral stelliplanate Pa element is distinguished from *Y. crassus sensu stricto* by a wider angle between the posterior and postero-lateral processes (45° vs 30–35°) and narrower platform ledges. **M**, *Yangtzeplacognathus crassus* (Chen & Zhang), dextral Pa (LY14-1, LO 12455t). **N**, *Yangtzeplacognathus crassus* (Chen & Zhang), sinistral Pb (LY14-1, LO 12456t). **O**, *Yangtzeplacognathus crassus* (Chen & Zhang), sinistral Pb (LY12-37, LO 12457t). **P**, *Yangtzeplacognathus crassus* (Chen & Zhang), sinistral Pa (LY12-34, LO 12458t). **Q**, *Baltoniodus medius* (Dzik), Sc (LY12-33, LO 12459t). **R**, *Baltoniodus medius* (Dzik), Pa (LY14-1, LO 12460t). **S**, *Baltoniodus medius* (Dzik), Sb, advanced specimen (LY14-1, LO 12461t). **T**, *Baltoniodus medius* (Dzik), Sc (LY14-1, LO 12462t). **U**, *Dzikodus hunanensis* Zhang, dextral Pa (LY14-5, LO 12463t). **V**, *Drepanoistodus basiovalis* (Sergeeva), M (LY12-31, LO 12464t). **W**, *Drepanoistodus basiovalis* (Sergeeva), M, pathological specimen with a damaged and self-repaired cusp (LY12-31, LO 12465t). **X**, *Lenodus pseudoplanus* (Viira), dextral Pa (LY12-42, LO 12466t). **Y**, *Lenodus pseudoplanus* (Viira), sinistral Pb (LY12-42, LO 12467t). **Z**, *Lenodus pseudoplanus* (Viira), sinistral Pb (LY12-42, LO 12468t). **AA**, *Lenodus pseudoplanus* (Viira), M (LY12-42, LO 12469t). **AB**, *Ansella* sp. (Löfgren), Sc (LY12-42, LO 12470t). **AC**, *Dapsilodus viruensis* (Fåhræus), acodontiform element (LY12-42, LO 12471t).

(2016), which was based on bed-by-bed macrofossil biofacies analyses and scaled in numeric terms by the tracking of limestone development in Baltoscandia. The glauconite-rich strata of the Volkhov Formation at the Lynna River appear to represent relatively deep water, with overall ~normal marine conditions (Fig. 4), although the conditions were clearly shallower than is typical for the distal parts of the Baltoscandian platform (or, large-scale ramp). The Volkhov–Kunda boundary coincides with a marked gap in the local depositional record (Fig. 4). This surface has been interpreted as a sequence boundary, and the overlying glauconite-speckled beds can be interpreted as transgressive lag deposits (Dronov et al. 1995; Dronov 1997c, 2013, 2017; Dronov & Holmer 1999; Iskyul 2004). The change to distinctly argillaceous facies in the Kunda reflects a drop in sea level, as evidenced both by sedimentary and faunal data, with enhanced terrestrial weathering and subsequent seaward transport of terrigenous matter. Thus, this interval was characterized by extensive mudflat-like areas and intermittent and patchy carbonate production in the East Baltic while oceanward parts of the Baltoscandian basin saw the establishment of relatively stable carbonate production (e.g., Lindström & Vortisch 1983; Olgun 1987; Nielsen 2004; Hints et al. 2012; Pärnaste et al. 2013; Lindskog & Eriksson 2017). The change into more argillaceous strata is notably accompanied by an increased abundance of ostracods, which may represent meiofauna living in soft substrates and turbid conditions unsuitable for many other benthic organisms (e.g., Hulings & Gray 1971). Perhaps there was some influence on the fauna also from changes in salinity due to freshwater dilution; the internal lamination seen in some beds suggests tidal influence and/or somewhat restricted conditions (see also Tolmacheva et al. 2003).

Relatively low sea level appears to have persisted well into the Kunda and a distinct lowstand was reached in the upper *A. expansus* trilobite Zone. This is corroborated by multi-section data on both facies and fossils from different parts of the Baltoscandian paleobasin, although details in relative sea level curves vary locally (e.g., Olgun 1987; Nordlund 1989; Nielsen 1995, 2004, 2011; Rasmussen & Stouge 1995, 2018; Karis 1998; Rasmussen et al. 2009, 2016; Männik & Viira 2012; Lindskog 2014; Lindskog et al. 2014, 2018, 2019; Lindskog & Eriksson 2017; and references therein). Iskyul (2015) described the interval spanning the *A. expansus* and basal *A. raniceps* beds at the nearby Lava River as 'ultra condensed', and this interval is commonly (very) thin or missing at the regional scale (e.g., Lamansky 1905; Jaanusson & Mutvei 1951; Mägi 1984; Raukas & Teedumäe 1997; Viira et al. 2001; Löfgren 2003; Rasmussen & Harper 2008; Rasmussen et al. 2009; Hints et al. 2012; Pärnaste et al. 2013). Similarly, gaps and signs of condensation and low sea level characterize coeval successions in many areas globally (e.g., Bunker et al. 1988; Young 1992; Barnes et al. 1996; Haq & Schutter 2008; and references therein). The hematite-enrichment in the uppermost *A. expansus* Zone is a regionally developed feature, possibly caused by increased microbial activity during reduced sedimentation rates (Lindskog 2014; Rozhnov 2017; Lindskog et al. 2018; and references therein). The boundary between the Lynna and Sillaoru formations clearly marks a break in sedimentation. This boundary has been interpreted as a transgressive surface and the boundary between the lowstand ($B_{III}\alpha$) and highstand ($B_{III}\beta$) systems tracts of the Kunda depositional sequence (Dronov & Holmer 1999; Dronov 2000, 2013; Rasmussen et al. 2009). The sediment-filled cavities in the topmost bed of the Lynna Formation appear to have been secondarily corroded and are closely similar to such interpreted as epikarst in other rock successions (e.g., Calner 2002; Jarochowska et al. 2016; and references therein). Hence, these features may be due to subaerial exposure, but unambiguous indicators of such conditions are missing and corrosion due to extended exposure at the seafloor cannot be excluded (whatever the case, the condensed nature of the rocks counteracts the preservation of many diagnostic features). The characteristics of overlying marl beds are in part similar to those of paleosols, but strong diagenetic alteration precludes detailed assessment (e.g., Tabor et al. 2017). It has been suggested that the marl beds are related to volcanism, as is perhaps also the case for the ferruginous debris found in this interval (see Sturesson et al. 1999; Sturesson 2003). Volcanically derived deposits occur in coeval strata at least in Sweden (e.g., Bergström 1989; Stouge & Nielsen 2003; Lindskog et al. 2017). The many hardgrounds and stained skeletal grains in the uppermost Lynna Formation and basal Sillaoru Formation indicate severe sedimentary condensation (*sensu* Föllmi 2016) of this part of the rock succession, which may help to explain the exceptional amounts of extraterrestrial chromite and other heavy minerals found in these beds as compared to correlative beds at other localities (see Lindskog et al. 2012). There is a consistently strong and statistically significant correlation ($r = 0.70 \pm 0.02$, $p < 0.05$) between different heavy mineral grain types, likely due to hydrodynamic concentration and sorting processes acting at the ancient seafloor (Fig. 4; ibid.). Similar covariance between extraterrestrial chromite and terrestrial heavy minerals is suggested in correlative strata at other localities (e.g., Schmitz & Häggström 2006; Häggström & Schmitz 2007), although this remains to be properly studied from sedimentologic perspectives (but see Alexeev 2014).

Sea level increased again in the mid-Kunda (transgression T3 *sensu* Rasmussen & Stouge 1995, transgressive systems tract *sensu* Dronov & Holmer 1999,

Basal Llanvirn Drowning Event *sensu* Nielsen 2004, initial Tableheadian transgression *sensu* Stouge et al. 2019) and brought with it a more stable marine environment. The 'White bed' at the top of the succession at the Lynna River is somewhat enigmatic, as it contains a peculiar mixture of both deeper- and shallower-water indicators (possibly due to condensation; see Föllmi 2016). Comparisons at the regional scale suggest that these strata represent the onset of a distinct shallowing in sea level, and data from the East Baltic show this to represent the shallowest phase of all of the Middle Ordovician succession in Baltoscandia (and the greater part of the Ordovician System) which can be correlated globally (Haq & Schutter 2008; Rasmussen et al. 2016; Lindskog & Eriksson 2017). This interval, termed 'regression R4' by Rasmussen & Stouge (1995), continued into the lower part of the *Microzarkodina ozarkodella* Subzone of the *L. pseudoplanus* conodont Zone on the distal part of the Baltoscandian shelf. The 'White bed' forms part of the highstand systems tract of the Kunda depositional sequence *sensu* Dronov & Holmer (1999).

Conodonts, and their paleoenvironmental and regional stratigraphic significance

The conodont fauna at the Lynna River clearly belongs to the *Baltoniodus–Microzarkodina* Biofacies of Rasmussen & Stouge (2018), which typified vast parts of the proximal Baltoscandian platform during the Middle Ordovician. Distal shelf or deep-water indicators such as *Periodon*, *Nordiora*, *Gothodus*, *Costiconus* and *Protopanderodus* are absent or very rare throughout the Lynna River section. Consequently, the very distinct changes in sea level that have been documented based on vertical variations in conodont biofacies from the Middle Ordovician succession on the distal parts of the Baltoscandian epeiric sea (Rasmussen & Stouge 1995) are not recognizable here.

Nearly all of the outcropping Volkhov Formation at the Lynna River belongs to the *Asaphus lepidurus* trilobite Zone (~*Megistaspis limbata* Zone westward; Hansen & Nielsen 2003; Ivantsov 2003; Pärnaste et al. 2013), confirming that this at least in part overlaps with the *L. antivariabilis* Zone (and the *Baltoniodus norrlandicus* Zone *sensu* Löfgren 2000a). The base of the *A. expansus* trilobite Zone is the classic indicator of the base of the Kunda Regional Stage (e.g., Ivantsov 2003, and references therein). At the Lynna River, the base of the *L. variabilis* conodont Zone is placed very close to, but immediately below, the *A. lepidurus–A. expansus* boundary. This is in good agreement with the zonal relationship in coeval sections across Baltica, but it can be noted that it varies slightly between localities. For example, at Slemmestad, Oslo region, Norway, the base of the *L. variabilis* Zone was placed *c*. 50 cm below the base of the *A. expansus* Zone (Rasmussen 1991; Nielsen 1995; Rasmussen et al. 2013), at Lanna, Närke, Sweden, it is *c*. 30 cm below (Löfgren 1995; Lindskog et al. 2018) and at Fågelsång, Scania, Sweden, it is *c*. 10 cm below (Stouge & Nielsen 2003). In several other localities, the base of the *L. variabilis* Zone closely overlies the base of the *A. expansus* Zone. For example, it occurs *c*. 15 cm above at Hagudden, Öland, Sweden (Stouge & Bagnoli 1990) and *c*. 10 cm above in the Finngrundet drill core, Sweden (Tjernvik & Johansson 1980; Löfgren 1985). At Kinnekulle, Västergötland, Sweden, the *L. variabilis* Zone has uncharacteristically been placed nearly 2 m into the *A. expansus* Zone, which there has a similar thickness as at the Lynna River (Zhang 1998b; Villumsen et al. 2001; Lindskog et al. 2014). The differences in the first occurrence of faunas typical of the *A. expansus* and *L. variabilis* zones between different localities may in large part be explained by variations in sample size and spacing, and/or local paleoenvironmental conditions. With regard to the latter and with specific importance for the eponymous zonal index taxa, it was indicated by Nielsen (1995), Hansen & Nielsen (2003) and Rasmussen et al. (2016) that *Asaphus* preferred relatively shallow-water conditions, and this was also clearly the case concerning *Lenodus* and *Eoplacognathus* during the early and middle Darriwilian as shown by Rasmussen & Stouge (2018). Hence, biozones defined on species belonging to these genera may be expected to vary stratigraphically to a certain degree from one locality to another, especially if the localities represent distinctly different paleoenvironmental conditions, and the common rarity and obviously diachronous appearance of the index taxa clearly illustrate the need to assess fossil faunas at the assemblage level to adequately tie strata together at the regional (and global) scale. Still, at least in the case of trilobite zones, the coincident patterns in the regional sedimentary development (see above) indicate that the zonal boundaries are essentially coeval within the temporal resolution offered by the geologic record. Taking into account the obvious surface of non-deposition that marks the Volkhov–Kunda boundary (basal unconformity of the Kunda depositional sequence *sensu* Dronov & Holmer 1999) at the Lynna River, and its rough topography, the bases of the *A. expansus* and *L. variabilis* zones can be considered as coincident locally.

The close coincidence between the base of the *Y. crassus* conodont Zone and that of the *A. raniceps* trilobite Zone is similar to what is seen in other places regionally; however, as is the case for the *A. expansus* and *L. variabilis* zones, the relative positions of the boundaries may vary slightly between localities (e.g., Nielsen 1995; Zhang 1997; Villumsen et al. 2001; Stouge & Nielsen 2003; Wu et al. 2018). The species *Y. crassus* appears to be somewhat problematic to use for detailed correlations between localities, both within Baltoscandia and else-

where, as this species was a temporary 'visitor' seemingly tracing transgressive strata (Stouge et al. 2019) and is ambiguous to identify (see Mellgren 2011).

Overall, the identification of conodont taxa typical of the North Atlantic faunal realm enables more robust correlations at both the regional and global scales (e.g., Gradstein et al. 2012, and references therein).

Dolomite and dolomitization

The characteristics of dolomite crystals in the samples from the Lynna River indicate formation during low-temperature conditions (<~50°; e.g., Sibley & Gregg 1987). In concert with the low CAI values of conodonts, and well-preserved oxygen-isotope and trace element concentrations in brachiopod shells (see Rasmussen et al. 2016), this indicates that the rocks have endured little post-depositional heating. Dolomite formation in sedimentary environments remains a contentious issue that is well beyond the scope of this paper (e.g., Gregg et al. 2015, and references therein). Whatever process(es) was/were behind the dolomitization at the Lynna River, burrows and borings clearly formed loci and preferential conduits for solutions that precipitated dolomite and fine-grained siliciclastics likely helped supply necessary magnesium ions. The dolomitization of burrows may be a result of microbial activity (Gingras et al. 2004). There is no immediately obvious connection between dolomitization and other documented proxies, but the most heavily dolomitized beds tend to be those marking transgressive pulses (especially such following upon distinct lowstands) and/or intervals with decreased sedimentation rates, and the stratigraphic patterns appear rhythmic/cyclic (Fig. 4). Volcanism may have played an important part in the dolomitization of the rocks, as volcanic ash provided abundant material that released magnesium ions upon weathering and during diagenesis (see above; e.g., Callen & Hermann 2019). In general, the proportion of dolomitized strata tends to increase westward along the Baltic–Ladoga Klint, but this pattern does not extend into western Estonia and beyond (e.g., Zaitsev & Kosorukov 2008). The dolomitization of the regional rock succession has commonly been interpreted as a Devonian phenomenon, although detailed studies indicate that this recrystallization (at least locally) was early diagenetic and closely tied to the depositional environment (e.g., Selivanova & Kofman 1971; Teedumäe et al. 2006; Plado et al. 2010; and references therein). The selective and partly localized dolomitization at the Lynna River suggests an early diagenetic origin, but it may very well be that there were several phases of dolomitization throughout geologic time. Any deeper analysis of spatiotemporal patterns in dolomitization relative to paleoenvironmental and/or diagenetic variations requires more detailed studies of the dolomite characteristics and systematic collection of data also from other localities.

Lynna River in the context of the GOBE

As already mentioned above, the sedimentary succession exposed at the Lynna River spans a key interval of the GOBE. Overall, at the global scale, the Volkhov–Kunda stages span a time when the so-called Paleozoic Evolutionary Fauna rapidly began to dominate ecosystems worldwide (Sepkoski 1981, 1995; Webby et al. 2004; Stigall et al. 2019; and references therein). The earliest Darriwilian was apparently characterized by an increased diversification rate among all metazoans (Kröger et al. 2019). This Middle Ordovician rise in biodiversity is notably evident within the suspension-feeding benthos, and particularly rhynchonelliformean brachiopods experienced a massive radiation at this time (Harper et al. 2013; Trubovitz & Stigall 2016; Colmenar & Rasmussen 2018; Hints et al. 2018). Rasmussen et al. (2007) constrained the main speciation phase among brachiopods to the late Dw1 and earliest Dw2 time slices (see Bergström et al. 2009), which translates into the *A. expansus–A. raniceps* interval of the regional trilobite zonation. However, much of these data originate from the significantly more condensed sections westward of the Lynna River (Lava River canyon and Putilovo Quarry), where the *A. expansus* Zone only reaches thicknesses of *c*. 0.5–0.7 m. The expanded Lynna River section, where this zone is more than 3 m thick, allows for a better-resolved stratigraphic/temporal understanding of the main phase of the GOBE. Brachiopod species level data at bed-by-bed resolution have been published separately for the Volkhov and Kunda parts of the local succession (Hansen & Harper 2003; Rasmussen & Harper 2008). These two data sets are combined herein, which allows for a range-interpolated brachiopod richness estimate through the Volkhov–Kunda transition and most of the succession at the Lynna River. Additionally, a range-interpolated species richness curve was compiled based on the conodont data presented herein (Fig. 6). For completeness, also a trilobite species richness curve was compiled based on data from Hansen & Nielsen (2003), although this only spans the Volkhov and basal Kunda beds. Together, these records enable direct comparisons of local species richness with other abiotic and biotic data at high stratigraphic resolution and provide added insight into the dynamics of the GOBE among key sessile benthos and nektobenthos.

Brachiopods show relatively stable species richness through the upper Volkhov at the Lynna River, with a gentle long-term trend of declining species numbers in the basal Kunda (Fig. 4). Approximately 0.8 m into the *A. expansus* Zone, brachiopods show an increase in species

numbers of more than 30% across an interval spanning only a few beds in the local succession (*c*. 0.5 m). Species richness remains high in the basal *A. raniceps* Zone, where it declines somewhat; however, this trend is at least in part exaggerated due to the range interpolation of the data (i.e., the range-through calculations do not include ranges of taxa stratigraphically above, yielding an apparent loss of richness). Most of the brachiopod richness development can be described as due to successive accumulation of species through time, but a few levels and intervals stand out in terms of species appearance and/or disappearance locally (Fig. 4; see Hansen & Harper 2003, fig. 7; Rasmussen & Harper 2008, fig. 4). Excluding the lowermost and uppermost portions of the data (which are inherently skewed by the range interpolation), these are: (1) the Volkhov–Kunda boundary interval, with equal numbers among appearances and disappearances; (2) the ~middle-third portion of the *A. expansus* trilobite Zone leading into the first species richness peak as discussed above, wherein a number of new taxa appeared whereas others disappeared; (3) the uppermost *A. expansus* Zone, characterized mainly by the appearance of numerous new species, but also the disappearance of others; (4) the basal *A. raniceps* Zone, wherein the disappearance of taxa clearly outpaces appearances.

Overall, brachiopod species richness appears to have been influenced by facies and/or water depth, and a preference for relatively shallow water is suggested by the regional species richness patterns (see Rasmussen et al. 2009). The interval that leads into the first main richness peak in the *A. expansus* Zone is characterized by contrasting signals in the inferred sea level curve based on different proxies at the Lynna River (about –2.25 to –1.75 m interval in Fig. 4). This is likely caused by mixing of faunal and sedimentary elements due to a minor gap or slowed sedimentation rates just prior to and during the onset of the positive species trend, as is revealed by the microfacies data through changes in the patterns of carbonate textures and fossil grain assemblages, and the amount of dolomitization (i.e. diagenetic influence on the strata). Hence, although the increase in brachiopod species richness was very rapid in terms of geologic time perspectives (e.g., Stigall et al. 2019), the apparent 'speciation' rates (i.e., addition of taxa per time unit) at the onset of the high diversity interval at the Lynna River may be slightly exaggerated by condensation effects. Curiously, this interval is also marked by a dip in $\delta^{13}C$ (possibly due to a significant proportion of 'old' carbon in reworked weathering materials). Regionally, a temporary break or change in the sedimentation rate at a closely coeval stratigraphic level, which coincides approximately with the peak of the basal Kunda transgression, is suggested by both macro- and micro-lithologic characteristics also at other localities. For example, at the Hällekis quarry, Västergötland, Sweden, a remarkably flat discontinuity surface is found in this interval, across which there is a notable change in microfacies characteristics similar to those at the Lynna River (Lindskog et al. 2014; Lindskog & Eriksson 2017). Prominent (and commonly ~planar) discontinuity surfaces occur at a similar stratigraphic level also at Hagudden (Nielsen 1995, and references therein), Gillberga (Löfgren 2000b) and Grönhögen (Ahlberg et al. 2019), Öland, and Lanna, Närke (Lindskog et al. 2018), as well as other areas in Sweden (A. Lindskog, unpublished). Clearly, this stratigraphic level represents a time of significant changes in the regional succession. A lack of comparable high-resolution data from localities outside the East Baltic (Rasmussen et al. 2007) precludes any detailed discussion on regional brachiopod richness records, although the Kunda Stage is commonly associated with increased species richness compared to older strata (e.g., Lindström 1971; Jaanusson 1982b; Jaanusson & Mutvei 1982; Hints et al. 2018).

Conodonts show largely stable species richness values through the Volkhov and species numbers then increase close to the Volkhov–Kunda boundary at the Lynna River (Figs 4, 6). The initial increase in richness is in part artificial, however, due to the temporary occurrence of long-ranging taxa. Species richness remains relatively high through the *L. variabilis* Zone and in the 'uncertain interval', where maximum species richness was reached before declining markedly through the *Y. crassus* Zone and ultimately reaching an overall low. Three intervals stand out in the data set: (1) the basal *L. variabilis* Zone, wherein a number of new species appeared; (2) the basal 'uncertain interval', where further new species appeared; (3) the *Y. crassus* Zone, which records a steady disappearance of taxa leading to the lowest species richness numbers of the entire studied succession.

In the East Baltic area, the upper Volkhov–middle Kunda interval appears to mainly be characterized by relatively low species richness among conodonts, but a long-term positive trend is then seen upward (e.g., Mägi 1984; Männik & Viira 2012). Stratigraphic patterns in conodont species richness through the Volkhov–Kunda interval clearly vary between localities in Baltoscandia, suggesting a strong influence from facies, water depth and possibly ocean currents (compare with discussion on biozonation above; e.g., Mägi 1984; Zhang 1998b; Viira et al. 2001; Viira 2011; Eriksson et al. 2012; Hints et al. 2012; Männik & Viira 2012; Rasmussen & Stouge 2018; Wu et al. 2018). At the global scale, conodont species richness began to rise early in the Ordovician and reached a distinct peak during the Floian, and a second less prominent peak occurred during the early to middle Darriwilian (Dw1–Dw2; e.g., Wu et al. 2012; Stouge et al. 2019; and references therein).

Trilobite species-level data from the Lynna River show relatively high richness through most of the *A. lepidurus* Zone (upper Volkhov), but a consistent decrease occurs through the uppermost *c*. 1 m of the zone and appears to continue into the *A. expansus* Zone (lower Kunda; Fig. 4). Unfortunately, there are not yet any detailed local data published from the Kunda interval and we therefore refrain from analyzing the trilobite data in any closer detail. At least among asaphids, the late Volkhov through Aseri interval is associated with a notable peak in overall richness and diversity in Baltoscandia (Pärnaste & Bergström 2013, fig. 5), and there was typically long-term increasing overall trilobite diversity during this time at the global scale (e.g., Adrain et al. 2004; Stigall et al. 2019).

Lateral variations in species richness highlight the need for assessing local data, which is sensitive to, for example, environmental and depositional conditions and sampling resolution, against carefully time-resolved regional richness patterns in order to attain a more complete picture. The species richness data from the Lynna River vary between fossil groups and do not consistently track any of the proxies documented herein, but sea level seems to have had some first-order influence on the local faunal development (Fig. 4). In light of the global boom in biodiversity during the studied time interval (e.g., Rasmussen et al. 2016, 2019; Kröger et al. 2019; Stigall et al. 2019), the overarching cause(s) of the species richness development (most apparent among brachiopods) is/are perhaps best sought beyond the local to regional scale. As discussed recently by, for example, Stigall et al. (2019), a number of factors and processes have been reasonably proposed to have had fundamental influence on biodiversity developments during the GOBE, including climate, oxygenation, volcanism, weathering and paleogeography. Kröger et al. (2019) showed that increased genus resilience was pivotal for stabilizing the ecosystems at this time so that biodiversity could begin to accumulate. Notably, the brachiopod species richness data from the relatively expanded succession at the Lynna River do not support any tangible connection between an enhanced influx of meteorites and biodiversification during the GOBE, as was speculated by Schmitz et al. (2008; cf. Lindskog et al. 2017) based on brachiopod diversity data from the East Baltic (Rasmussen et al. 2007) – the pronounced rise in brachiopod species richness in the early Kunda is clearly disjunct from the increase in extraterrestrial chromite close to the *A. expansus–A. raniceps* boundary, as well as from the Volkhov–Kunda boundary (Fig. 4; cf. Schmitz et al. 2008). Moreover, diachronous species richness patterns between and within faunal groups locally, regionally and globally are inconsistent with attribution to a discrete 'event'. Whatever phenomena may have influenced the biodiversity development, and their possible relationship(s) in-between, much scientific work remains to be done to further our understanding of this intriguing chapter in Earth history.

CONCLUSIONS

The macroscopic and microscopic characteristics of the strata at the Lynna River provide clues to the paleoenvironmental development during the Middle Ordovician. As it is relatively expanded, the local succession forms a key for more detailed comparisons to coeval strata outside the East Baltic. Microfacies commonly co-vary in a predictable manner with the macroscopic appearance of the rocks, with intervals characterized by competent limestone being associated with coarser carbonate textures and marl-rich nodular limestone intervals associated with finer textures. The changes in facies were strongly influenced by changes in sea level and the main stratigraphic patterns and 'event' levels are (at least) regionally traceable. The collective data suggest a trend of shallowing sea level from the late Volkhov through mid-Kunda interval (early Darriwilian), in agreement with regional and global scenarios. The local rocks are commonly partly dolomitized, but the precise timing and possible paleoenvironmental significance of the dolomitization remain to be studied in closer detail. Based on the conodont data presented herein, the regional East Baltic macrofossil biozonation can now be tied more robustly to global biostratigraphic frameworks. The conodont biozonation at the Lynna River section agrees well with regional biostratigraphic correlations traditionally based mainly on trilobites. The compilation of new and previously published fossil data shows that the early Kunda (Darriwilian, middle Dw1–early Dw2) records increase in species richness among sessile suspension-feeding benthos (brachiopods) and nekto-benthos (conodonts).

Acknowledgements. This study was funded by the Royal Physiographic Society in Lund and the Birgit and Hellmuth Hertz' Foundation (A. L.), the Swedish Research Council (M. E. E.), the Carlsberg Foundation (J. A. R.), the Regional Governmental Program of Competitive Growth of Kazan Federal University and Russian Foundation for Basic Research (grant N19-05-00748; A. D.) and GeoCenter Denmark (grants Nos 2015-5 and 3-2017; C. M. Ø. R.). Thanks are due to F. Terfelt for assistance during sampling and B. Schmitz for coordinating field work. G. Klintvik-Ahlberg and C. Tell are thanked for preparation of conodont samples, and J. Lindgren is thanked for providing photographic equipment. We thank Olle Hints and Björn Kröger for helpful reviews. This paper is a contribution to IGCP project 653 – 'The onset of the Great Ordovician Biodiversification Event.' The publication costs of this article were partially covered by the Estonian Academy of Sciences.

REFERENCES

Adrain, J. M., Edgecombe, G. D., Fortey, R. A., Hammer, Ø., Laurie, J. R., McCormick, T., Owen, A. W., Waisfeld, B. G., Webby, B. D., Westrop, S. R. & Zhou, Z.-Y. 2004. Trilobites. In *The Great Ordovician Biodiversification Event* (Webby, B. D., Droser, M. L. & Paris, F., eds), pp. 231–254. Columbia University Press, New York.

Ahlberg, P., Lundberg, F., Erlström, M., Calner, M., Lindskog, A., Dahlqvist, P. & Joachimski, M. M. 2019. Integrated Cambrian biostratigraphy and carbon isotope chemostratigraphy of the Grönhögen-2015 drill core, Öland, Sweden. *Geological Magazine*, **156**, 935–949.

Alexeev, V. A. 2014. Some features of distributions of extraterrestrial chromite grains in Ordovician limestone of the different regions of the world. In *45th Lunar and Planetary Science Conference Abstracts*, No. 1005. Lunar and Planetary Institute, Houston.

Alikhova, T. N. 1960. *Stratigrafiya ordovikskikh otlozhenij Russkoj platformy* [*Ordovician Stratigraphy of the Russian Platform*]. Gosgeoltekhizdat, Moscow, 76 pp. [in Russian].

Bagnoli, G. & Stouge, S. 1997. Lower Ordovician (Billingenian–Kunda) conodont zonation and provinces based on sections from Horns Udde, north Öland, Sweden. *Bollettino della Società Paleontologica Italiana*, **33**, 109–163.

Barnes, C. R., Fortey, R. A. & Williams, S. H. 1996. The pattern of global bio-events during the Ordovician Period. In *Global Events and Event Stratigraphy in the Phanerozoic* (Walliser, O. H., ed.), pp. 139–172. Springer-Verlag, Berlin.

Bergström, S. M. 1989. Use of graphic correlation for assessing event-stratigraphic significance and trans-Atlantic relationships of Ordovician K-bentonites. *Proceedings of the Academy of Sciences of the Estonian SSR, Geology*, **38**, 55–59.

Bergström, S. M., Chen, X., Guitiérrez-Marco, J. C. & Dronov, A. 2009. The new chronostratigraphic classification of the Ordovician System and its relations to major regional series and stages and to $\delta^{13}C$ chemostratigraphy. *Lethaia*, **42**, 97–107.

Bunker, B. J., Witzke, B. J., Watney, W. L. & Ludvigson, G. A. 1988. Phanerozoic of the central midcontinent, United States. In *Sedimentary Cover – North American Craton, The Geology of North America D-2* (Sloss, L. L., ed.), pp. 243–260. Geological Society of America, Boulder.

Callen, J. M. & Herrmann, A. D. 2019. In situ geochemistry of middle Ordovician dolomites of the upper Mississippi valley. *The Depositional Record*, **5**, 4–22.

Calner, M. 2002. A lowstand epikarstic intertidal flat from the middle Silurian of Gotland, Sweden. *Sedimentary Geology*, **148**, 389–403.

Cocks, L. R. M. & Torsvik, T. H. 2006. European geography in a global context from the Vendian to the end of the Palaeozoic. In *European Lithosphere Dynamics* (Gee, D. G. & Stephenson, R. A., eds*)*, pp. 83–95. Geological Society, London.

Colmenar, J. & Rasmussen, C. M. Ø. 2018. A Gondwanan perspective on the Ordovician Radiation constrains its temporal duration and suggests first wave of speciation, fuelled by Cambrian clades. *Lethaia*, **51**, 286–295.

Cronholm, A. & Schmitz, B. 2010. Extraterrestrial chromite distribution across the mid-Ordovician Puxi River section, central China: evidence for a global major spike in flux of L-chondritic matter. *Icarus*, **208**, 36–48.

Dronov, A. V. 1997a. Calcareous tempestites: depositional model for the Lower and Middle Ordovician of St. Petersburg region, NW Russia. In *WOGOGOB-97 Abstracts* (Koren, T. N., ed.), p. 21. VSEGEI, St. Petersburg.

Dronov, A. V. 1997b. Sea-level changes in the Ordovician of St. Petersburg region. In *WOGOGOB-97 Abstracts* (Koren, T. N., ed.), pp. 20–21. VSEGEI, St. Petersburg.

Dronov, A. V. (ed.). 1997c. Russian and International Bryozoan Conference, Bryozoa of the world: a field excursion guide, 30 June–8 July 1997, St. Petersburg. *Terra Nostra, Schriften der Alfred-Wegener-Stiftung*, **97**(12), 1–56.

Dronov, A. V. 1998. Shtormovaya sedimentatsiya v nizhneordovikskikh karbonatno-terrigennykh otlozheniyakh okrestnostej Sankt-Peterburga [Storm sedimentation in the Lower Ordovician mixed carbonate-terrigenous deposits in the vicinity of St. Petersburg]. *Byulleten' MOIP, Otdel Geologicheskij*, **73**(2), 43–51 [in Russian].

Dronov, A. V. 1999. Kolebaniya urovnya morya v rannem ordovike i ikh otrazhenie v razrezakh vostochnoj chasti glinta [The fluctuations of the sea level in the early Ordovician and their reflection in the sections of the eastern part of the glint]. *Byulleten' MOIP, Otdel Geologicheskij*, **74**, 39–47 [in Russian].

Dronov, A. V. 2000. *Sekvens-stratigrafiya ordovikskogo paleobassejna Baltoskandii, Avtoreferat na soiskanie uchenoj stepeni doktora geologo-mineralogicheskikh nauk* [*Sequence Stratigraphy of the Ordovician Paleobasin of Baltoscandia, Summary of the Dr of Science Dissertation*]. St. Petersburg University, St. Petersburg, 32 pp. [in Russian].

Dronov, A. V. 2013. Depositional sequences and sea-level changes in the Ordovician of Baltoscandia. In *Stratigraphy of the Early XXI Century: Tendencies and New Ideas* (Gladenkov, Yu. B. & Mezhelovskii, N. V., eds), pp. 65–92. Geokart, GEOS, Moscow [in Russian].

Dronov, A. 2017. Chapter 5 – Ordovician sequence stratigraphy of the Siberian and Russian platforms. In *Advances in Sequence Stratigraphy. Special Issue: Stratigraphy & Timescale, Vol. 2* (Montenari, M., ed.), pp. 187–241. Elsevier, Oxford.

Dronov, A. V. & Fedorov, P. V. 1995. Karbonatnyj ordovik okrestnostej S.-Peterburga: stratigrafiya zheltyakov i frizov [Carbonate Ordovician in the Vicinity of St. Petersburg: Stratigraphy of Zheltiaki and Frizy]. *Vestnik St.-Peterburgskogo Uuniversiteta*, *Vyp. 7*: *Geologiya, Geografiya, Vyp. 2*, **14**, 9–16 [in Russian].

Dronov, A. & Holmer, L. E. 1999. Depositional sequences in the Ordovician of Baltoscandia. In *Quo vadis Ordovician? Short Papers of the 8th International Symposium on the Ordovician System* (Kraft, P. & Fatka, O., eds), *Acta Universitatis Carolinae – Geologica,* **43**, 1133–1136.

Dronov, A. & Holmer, L. 2002. Ordovician sea-level curve: Baltoscandian view. In *The Fifth Baltic Stratigraphical Conference, Basin Stratigraphy – Modern Methods and Problems, September 22–27, 2002, Vilnius, Lithuania:*

Extended Abstracts (Satkūnas, J. & Lazauskienė, J., eds), pp. 33–35. Vilnius Universtiy, Vilnius.

Dronov, A. & Mikuláš, R. 2010. *Paleozoic Ichnology of St. Petersburg Region: Excursion Guidebook*. Geological Institute, Russian Academy of Sciences, Moscow, 70 pp.

Dronov, A. & Rozhnov, S. 2007. Climatic changes in the Baltoscandian basin during the Ordovician: sedimentological and palaeontological aspects. *Acta Palaeontologica Sinica*, **46**, S108–S113.

Dronov, A. V., Koren, T. N., Popov, L. E., Tolmacheva, T. Yu. & Holmer, L. E. 1995. Uppermost Cambrian and Lower Ordovician in northwestern Russia: sequence stratigraphy, sea level changes and bio-events. In *Ordovician Odyssey: Short Papers for the Seventh International Symposium on the Ordovician System* (Cooper, J. D., Droser, M. L. & Finney, S. C., eds), *Pacific Section, Society for Sedimentary Geology (SEPM)*, **77**, 319–322.

Dronov, A. V., Koren, T. N., Popov, L. E. & Tolmacheva, T. Yu. 1998. *Metodika sobytijnoj stratigrafii v obosnovanii korrelyatsii regional'nykh stratonov na primere nizhnego ordovika Severo-Zapada Rossii* [*Methodology of Event Stratigraphy in the Justification of Regional Stratigraphic Correlations on the Example of the Lower Ordovician of Northwest Russia*]. Izd-vo VSEGEI, St. Petersburg, 88 pp. [in Russian].

Dronov, A., Holmer, L., Meidla, T., Sturesson, U., Tinn, O. & Ainsaar, L. 2001. Detailed litho- and sequence stratigraphy of the "Täljsten" limestone unit and its equivalents in the Ordovician of Baltoscandia. In *WOGOGOB-2001 Abstracts* (Harper, D. A. T. & Stouge, S., eds), pp. 8–9. Copenhagen University, Copenhagen.

Dronov, A. V., Mikuláš, R. & Logvinova, M. 2002. Trace fossils and ichnofabrics across the Volkhov depositional sequence (Ordovician, Arenigian of St. Petersburg region, Russia). *Journal of the Czech Geological Society*, **47**, 133–146.

Dronov, A., Tolmacheva, T., Raevskaya, E. & Nestell, M. (eds). 2005. *Cambrian and Ordovician of St. Petersburg Region*. St. Petersburg State University, St. Petersburg, 62 pp.

Dronov, A. V., Ainsaar, L., Kaljo, D., Meidla, T., Saadre, T. & Einasto, R. 2011. Ordovician of Baltoscandia: facies, sequences and sea-level changes. In *Ordovician of the World* (Gutiérrez-Marco, J. C., Rábano, I. & Garcia-Bellido, D., eds), *Publicaciones del Instituto Geológico y Minero de España, Cuadernos del Museo Geominero*, **14**, 143–150.

Dunham, R. J. 1962. Classification of carbonate rocks according to depositional texture. In *Classification of Carbonate Rocks – A Symposium* (Ham, W. E., ed.), *American Association of Petroleum Geologists Memoir*, **1**, 108–121.

Epstein, A. G., Epstein, J. B. & Harris, L. D. 1977. Conodont color alteration – an index to organic metamorphism. *Geological Survey Professional Paper*, **995**, 1–27.

Eriksson, M. E., Lindskog, A., Calner, M., Mellgren, J. I. S., Bergström, S. M., Terfelt, F. & Schmitz, B. 2012. Biotic dynamics and carbonate microfacies of the conspicuous Darriwilian (Middle Ordovician) 'Täljsten' interval, south-central Sweden. *Palaeogeography, Palaeoclimatology, Palaeoecology*, **367–368**, 89–103.

Flügel, E. 2010. *Microfacies of Carbonate Rocks: Analysis, Interpretation and Application*. Springer Verlag, Berlin, 984 pp.

Föllmi, K. B. 2016. Sedimentary condensation. *Earth-Science Reviews*, **152**, 143–180.

Gingras, M. K., Pemberton, S. G., Muelenbachs, K. & Machel, H. 2004. Conceptual models for burrow-related, selective dolomitization with textural and isotopic evidence from the Tyndall Stone, Canada. *Geobiology*, **2**, 21–30.

Gradstein, F. M., Ogg, J. G., Schmitz, M. D. & Ogg, G. M. (eds). 2012. *The Geologic Time Scale 2012*. Elsevier, Boston, 1176 pp.

Gregg, J. M., Bish, D. L., Kaczmarek, S. E. & Machel, H. G. 2015. Mineralogy, nucleation and growth of dolomite in the laboratory and sedimentary environment: a review. *Sedimentology*, **62**, 1749–1769.

Häggström, T. & Schmitz, B. 2007. Distribution of extraterrestrial chromite in Middle Ordovician Komstad Limestone in the Killeröd quarry, Scania, Sweden. *Bulletin of the Geological Society of Denmark*, **55**, 37–58.

Hansen, J. & Harper, D. A. T. 2003. Brachiopod macrofaunal distribution through the upper Volkhov–lower Kunda (Lower Ordovician) rocks, Lynna River, St. Petersburg region. *Bulletin of the Geological Society of Denmark*, **50**, 45–53.

Hansen, T. & Nielsen, A. T. 2003. Upper Arenig trilobite biostratigraphy and sea-level changes at Lynna River near Volkhov, Russia. *Bulletin of the Geological Society of Denmark*, **50**, 105–114.

Harper, D. A. T., Rasmussen, C. M. Ø., Liljeroth, M., Blodgett, R. B., Candela, Y., Jin, J., Percival, I. G., Rong, J.-Y., Villas, E. & Zhan, R.-B. 2013. Biodiversity, biogeography and phylogeography of Ordovician rhynchonelliform brachiopods. *Geological Society, London, Memoirs*, **38**, 127–144.

Harper, D. A. T, Hammarlund, E. U. & Rasmussen, C. M. Ø. 2014. End Ordovician extinctions: a coincidence of causes. *Gondwana Research*, **25**, 1294–1307.

Haq, B. & Schutter, S. R. 2008. A chronology of Paleozoic sea-level changes. *Science*, **322**, 64–68.

Heck, P. R., Schmitz, B., Rout, S. S., Tenner, T., Villalon, K., Cronholm, A., Terfelt, F. & Kita, N. T. 2016. A search for H-chondritic chromite grains in sediments that formed immediately after the breakup of the L-chondrite parent body 470 Ma ago. *Geochimica et Cosmochimica Acta*, **177**, 120–129.

Heck, P. R., Schmitz, B., Bottke, W. F., Rout, S. S., Kita, N. T., Cronholm, A., Defouilloy, C., Dronov, A. & Terfelt, F. 2017. Rare meteorites common in the Ordovician period. *Nature Astronomy*, **1**, 0035.

Hints, L., Harper, D. A. T. & Paškevičius, J. 2018. Diversity and biostratigraphic utility of Ordovician brachiopods in the East Baltic. *Estonian Journal of Earth Sciences*, **67**, 176–191.

Hints, O., Viira, V. & Nõlvak, J. 2012. Darriwilian (Middle Ordovician) conodont biostratigraphy in NW Estonia. *Estonian Journal of Earth Sciences*, **61**, 210–226.

Hulings, N. C. & Gray, J. S. 1971. A manual for the study of meiofauna. *Smithsonian Contributions to Zoology*, **78**, 1–83.

Iskyul, G. S. 2004. Sekvens-stratigraficheskoe raschlenenie intervala $B_{III}\alpha$–$B_{III}\beta$ kundaskogo gorizonta (ordovik) Leningradskoj oblasti [Sequence stratigraphy of the $B_{III}\alpha$–$B_{III}\beta$ interval of the Kunda Regional Stage (Ordovician) of the Leningrad region]. In *Ordovikskoe plato (k 100-letiyu so dnya rozhdeniya B. P. Asatkina. Nauchnye chteniya po geologii ordovika Leningradskoj oblasti* [*Ordovician Plateau (100 years from the Birthday of B. P. Asatkin. Scientific Reading on the Ordovician Geology of the Leningrad Region)*] (Dronov, A. V., ed.), pp. 68–85. Voentekhinizdat, Moscow [in Russian].

Iskyul, G. S. 2015. Opornyj razrez kundaskogo gorizonta (srednij ordovik) na reke Lava: opisanie i biostratigraficheskoe raschlenenie po trilobitam [Key section of the Kunda Regional Stage (Middle Ordovician) at the Lava River: description and biostratigraphy based on trilobites]. *Regional'naya Geologiya i Metallogeniya* [*Regional Geology and Metallogeny*], **63**, 9–19 [in Russian, with English summary].

Ivantsov, A. Yu. 2003. Ordovician trilobites of the subfamily Asaphinae of the Ladoga Glint. *Paleontological Journal*, **37**, S229–S337.

Ivantsov, A. Yu. & Melnikova, L. M. 1998. Volkhovskij i kundaskij gorizonty ordovika i kharakteristika trilobitov i ostrakod na reke Volkhov (Leningradskaya oblast′) [Ordovician Volkhov and Kunda regional stages and characteristics of trilobites and ostracods on the Volkhov River (Leningrad Region)]. *Stratigrafiya. Geologicheskaya korrelyatsiya* [*Stratigraphy. Geologic Correlation*], **6**(5), 47–63 [in Russian].

Jaanusson, V. 1973. Aspects of carbonate sedimentation in the Ordovician of Baltoscandia. *Lethaia*, **6**, 11–34.

Jaanusson, V. 1976. Faunal dynamics in the Middle Ordovician (Viruan) of Baltoscandia. In *The Ordovician System: Proceedings of a Palaeontological Association Symposium, Birmingham, September 1974* (Bassett, M. G., ed.), pp. 301–326. University of Wales Press and National Museum of Wales, Cardiff.

Jaanusson, V. 1982a. Introduction to the Ordovician of Sweden. In *Field Excursion Guide. 4th International Symposium on the Ordovician System* (Bruton, D. L. & Williams, S. J., eds)*, Paleontological Contributions from the University of Oslo*, **279**, 1–10.

Jaanusson, V. 1982b. The Siljan district. In *Field Excursion Guide. 4th International Symposium on the Ordovician System* (Bruton, D. L. & Williams, S. J., eds), *Paleontological Contributions from the University of Oslo*, **279**, 15–42.

Jaanusson, V. 1995. Confacies differentiation and upper Middle Ordovician correlation in the Baltoscandian Basin. *Proceedings of the Estonian Academy of Sciences*, **44**, 73–86.

Jaanusson, V. & Mutvei, H. 1951. Ein Profil durch den Vaginatum-Kalkstein im Siljan-Gebiet, Dalarna. *Geologiska Föreningens i Stockholm Förhandlingar*, **73**, 630–636.

Jaanusson, V. & Mutvei, H. 1982. *Ordovician of Öland. Guide to Excursion 3. IV International Symposium on the Ordovician System, Oslo 1982*. Swedish Museum of Natural History, Stockholm, 23 pp.

Jarochowska, E., Munnecke, A., Frisch, K., Ray, D. C. & Castagner, A. 2016. Faunal and facies changes through the mid Homerian (late Wenlock, Silurian) positive carbon isotope excursion in Podolia, western Ukraine. *Lethaia*, **49**, 170–198.

Jeppsson, L., Anehus, R. & Fredholm, D. 1999. The optimal acetate buffered acetic acid technique for extracting phosphatic fossils. *Journal of Paleontology*, **73**, 957–965.

Karis, L. 1998. Jämtlands östliga fjällberggrund. In *Beskrivning till berggrundskartan över Jämtlands län, Del 2: Fjälldelen* (Karis, L. & Strömberg, A. G. B., eds), *Sveriges Geologiska Undersökning*, **Ca 53**(2), 1–184.

Knaust, D. & Dronov, A. 2013. *Balanoglossites* ichnofabrics from the middle Ordovician Volkhov formation (St. Petersburg region, Russia). *Stratigraphy and Geological Correlation*, **21**, 265–279.

Knaust, D., Curran, H. A. & Dronov, A. V. 2012. Shallow-marine carbonates. In *Trace Fossils as Indicators of Sedimentary Environments* (Knaust, D. & Bromley, R., eds), *Developments in Sedimentology*, **64**, 705–750.

Korochantsev, A. V., Lorenz, C. A., Ivanova, M. A., Zaytsev, A. V., Kononkova, N. N., Roshchina, I. A., Korochantseva, E. V., Sadilenko, D. A. & Skripnik, A. Yu. 2009. Sediment-dispersed extraterrestrial chromite in Ordovician limestone from Russia. In *Abstracts of Papers Submitted to the Lunar and Planetary Science Conference XL*, No. 1101.

Koromyslova, A. V. 2011. Bryozoans of the Latorp and Volkhov Horizons (Lower–Middle Ordovician) of the Leningrad Region. *Paleontological Journal*, **45**, 887–980.

Kröger, B. & Rasmussen, J. A. 2014. Middle Ordovician cephalopod biofacies and palaeoenvironments of Baltoscandia. *Lethaia*, **47**, 275–295.

Kröger, B., Franeck, F. & Rasmussen, C. M. Ø. 2019. The evolutionary dynamics of the early Palaeozoic marine biodiversity accumulation. *Proceedings of the Royal Society B*, **286**, doi: 10.1098/rspb.2019.1634.

Lamansky, W. 1905. Drevnejshie sloi silurijskikh otlozhenij Rossii [Die aeltesten silurischen Schichten Russlands (Etage B)]. *Trudy Geologicheskogo Komiteta, Novaya Seriya*/*Mémoires du Comité Géologique, Nouvelle Serie*, Livr. 20, 1–203 [in Russian, with German summary].

Lindskog, A. 2014. Palaeoenvironmental significance of cool-water microbialites in the Darriwilian (Middle Ordovician) of Sweden. *Lethaia*, **47**, 187–204.

Lindskog, A. & Eriksson, M. E. 2017. Megascopic processes reflected in the microscopic realm: sedimentary and biotic dynamics of the Middle Ordovician "orthoceratite limestone" at Kinnekulle, Sweden. *GFF*, **139**, 163–183.

Lindskog, A., Schmitz, B., Cronholm, A. & Dronov, A. 2012. A Russian record of a Middle Ordovician meteorite shower: extraterrestrial chromite at Lynna River, St. Petersburg region. *Meteoritics and Planetary Science*, **47**, 1274–1290.

Lindskog, A., Eriksson, M. E. & Pettersson, A. M. L. 2014. The Volkhov–Kunda transition and the base of the Holen Limestone at Kinnekulle, Västergötland, Sweden. *GFF*, **136**, 167–171.

Lindskog, A., Costa, M. M., Rasmussen, C. M. Ø., Connelly, J. N. & Eriksson, M. E. 2017. Refined Ordovician timescale reveals

no link between asteroid breakup and biodiversification. *Nature Communications*, **8**, 14066.

Lindskog, A., Lindskog, A. M. L., Johansson, J. V., Ahlberg, P. & Eriksson, M. E. 2018. The Cambrian–Ordovician succession at Lanna, Närke, Sweden: stratigraphy and depositional environments. *Estonian Journal of Earth Sciences*, **67**, 133–148.

Lindskog, A., Eriksson, M. E., Bergström, S. M. & Young, S. A. 2019. Lower–Middle Ordovician carbon and oxygen isotope chemostratigraphy at Hällekis, Sweden: implications for regional to global correlations and palaeoenvironmental development. *Lethaia*, **52**, 204–219.

Lindström, M. 1971. Vom Anfang, Hochstand und Ende eines Epikontinentalmeeres. *Geologische Rundschau*, **60**, 419–438.

Lindström, M. & Vortisch, W. 1983. Indications of upwelling in the Lower Ordovician of Scandinavia. In *Coastal Upwelling – Its Sediment Record, Part B: Sedimentary Records of Ancient Coastal Upwelling* (Thiede, J. & Suess, E., eds), pp. 535–551. Plenum Publishing, New York.

Löfgren, A. 1985. Early Ordovician conodont biozonation at Finngrundet, south Bothnian Bay, Sweden. *Bulletin of the Geological Institution of the University of Uppsala*, **10**, 115–128.

Löfgren, A. 1995. The middle Lanna/Volkhov Stage (middle Arenig) of Sweden and its conodont fauna. *Geological Magazine*, **132**, 693–711.

Löfgren, A. 2000a. Conodont biozonation in the upper Arenig of Sweden. *Geological Magazine*, **137**, 53–65.

Löfgren, A. 2000b. Early to early Middle Ordovician conodont biostratigraphy of the Gillberga quarry, northern Öland, Sweden. *GFF*, **122**, 321–338.

Löfgren, A. 2003. Conodont faunas with *Lenodus variabilis* in the upper Arenigian to lower Llanvirnian of Sweden. *Acta Palaeontologica Polonica*, **48**, 417–436.

Löfgren, A. 2004. The conodont fauna in the Middle Ordovician *Eoplacognathus pseudoplanus* Zone of Baltoscandia. *Geological Magazine*, **141**, 505–524.

Löfgren, A. & Zhang, J. 2003. Element association and morphology in some Middle Ordovician platform-equipped conodonts. *Journal of Paleontology*, **77**, 721–737.

Mägi, S. 1984. Kharakteristika stratotipa Ontikaskoj podserii [A characterization of the type section of the Ontika subseries]. *Proceedings of the Academy of Sciences of the Estonian SSR, Geology*, **33**, 104–112 [in Russian, with English summary].

Männik, P. & Viira, V. 2012. Ordovician conodont diversity in the northern Baltic. *Estonian Journal of Earth Sciences*, **61**, 1–14.

Männil, R. M. 1966. *Istoriya razvitiya Baltijskogo bassejna v ordovike* [*Evolution of the Baltic Basin during the Ordovician*]. Eesti NSV Teaduste Akadeemia Geoloogia Instituut, Tallinn, 199 pp. [in Russian with English summary].

Meier, M. M. M., Schmitz, B., Lindskog, A., Maden, C. & Wieler, R. 2014. Cosmic-ray exposure ages of fossil micrometeorites from mid-Ordovician sediments at Lynna River, Russia. *Geochimica et Cosmochimica Acta*, **125**, 338–350.

Mellgren, J. 2011. Conodont biostratigraphy, taxonomy and palaeoecology in the Darriwilian (Middle Ordovician) of Baltoscandia – with focus on meteorite and extraterrestrial chromite-rich strata. *Litholund Theses*, **21**, 1–130.

Mellgren, J. I. S. & Eriksson, M. E. 2010. Untangling a Darriwilian (Middle Ordovician) palaeoecological event in Baltoscandia: conodont faunal changes across the 'Täljsten' interval. *Earth and Environmental Science Transactions of the Royal Society of Edinburgh*, **100**, 353–370.

Mestre, A. & Heredia, S. 2017. New taxonomic insights on the conodont genus *Lenodus* (lower Darriwilian) from the Precordillera, San Juan, Argentina. In *Fourth International Conodont Symposium. ICOS IV. "Progress on Conodont Investigation"* (Liao, J.-C. & Valenzuela-Ríos, J. I., eds), *Cuadernos del Museo Geominero*, **22**, 49–53.

Nielsen, A. T. 1995. Trilobite systematics, biostratigraphy and palaeoecology of the Lower Ordovician Komstad Limestone and Huk formations, southern Scandinavia. *Fossils and Strata*, **38**, 1–374.

Nielsen, A. T. 2004. Ordovician sea level changes: a Baltoscandian perspective. In *The Great Ordovician Biodiversification Event* (Webby, B. D., Paris, F., Droser, M. L. & Percival, I. G., eds), pp. 84–93. Columbia University Press, New York.

Nielsen, A. T. 2011. A re-calibrated revised sea-level curve for the Ordovician of Baltoscandia. In *Ordovician of the World* (Gutiérrez-Marco, J. C., Rábano, I. & Garcia-Bellido, D., eds), *Publicaciones del Instituto Geológico y Minero de España, Cuadernos del Museo Geominero*, **14**, 399–401.

Nordlund, U. 1989. Lithostratigraphy and sedimentology of a Lower Ordovician limestone sequence at Hälludden, Öland, Sweden. *GFF*, **111**, 65–94.

Normore, L. S., Zhen, Y. Y., Dent, L. M., Crowley, J. L., Percival, I. G. & Wingate, M. T. D. 2018. Early Ordovician CA-IDTIMS U–Pb zircon dating and conodont biostratigraphy, Canning Basin, Western Australia. *Australian Journal of Earth Sciences*, **65**, 61–73.

Olgun, O. 1987. Komponenten-Analyse und Conodonten-Stratigraphie der Orthoceratenkalksteine im Gebiet Falbygden, Västergötland, Mittelschweden. *Sveriges Geologiska Undersökning*, **Ca 70**, 1–78.

Pander, C. H. 1830. *Beiträge zur Geognosie des Russischen Reiches*. Karl Kray, St. Petersburg, 165 pp.

Pärnaste, H. & Bergström, J. 2013. The asaphid trilobite fauna: its rise and fall in Baltica. *Palaeogeography, Palaeoclimatology, Palaeoecology*, **389**, 64–77.

Pärnaste, H., Bergström, J. & Zhou, Z. 2013. High resolution trilobite stratigraphy of the Lower–Middle Ordovician Öland Series of Baltoscandia. *Geological Magazine*, **150**, 509–518.

Plado, J., Preeden, U., Pesonen, L. J., Mertanen, S. & Puura, V. 2010. Magnetic history of Early and Middle Ordovician sedimentary sequence, northern Estonia. *Geophysical Journal International*, **180**, 147–157.

Põlma, L. 1982. *Sravnitel´naya litologiya karbonatnykh porod ordovika Severnoj i Srednej Pribaltiki* [*Comparative Lithology of Ordovician Carbonate Rocks in North and Central East Baltic*]. Valgus, Tallinn, 152 pp. [in Russian, with English summary].

Popov, L. E. (ed.). 1997. *WOGOGOB Excursion Guide: St. Petersburg, Russia, 1997*. Uppsala University, Uppsala, 24 pp. (+ figure appendix).

Powers, M. C. 1953. A new roundness scale for sedimentary particles. *Journal of Sedimentary Petrology*, **23**, 117–119.

Rasmussen, C. M. Ø. & Harper, D. A. T. 2008. Resolving early Mid-Ordovician (Kundan) bioevents in the East Baltic based on brachiopods. *Geobios*, **41**, 533–542.

Rasmussen, C. M. Ø., Hansen, J. & Harper, D. A. T. 2007. Baltica: a mid Ordovician diversity hotspot. *Historical Biology*, **19**, 255–261.

Rasmussen, C. M. Ø., Nielsen, A. T. & Harper, D. A. T. 2009. Ecostratigraphical interpretation of lower Middle Ordovician East Baltic sections based on brachiopods. *Geological Magazine*, **146**, 717–731.

Rasmussen, C. M. Ø., Ullmann, C. V., Jakobsen, K. G., Lindskog, A., Hansen, J., Hansen, T., Eriksson, M. E., Dronov, A., Frei, R., Korte, C., Nielsen, A. T. & Harper, D. A. T. 2016. Onset of main Phanerozoic marine radiation sparked by emerging Mid Ordovician icehouse. *Scientific Reports*, **6**, 18884.

Rasmussen, C. M. Ø., Kröger, B., Nielsen, M. L. & Colmenar, J. 2019. Cascading trend of Early Paleozoic marine radiations paused by Late Ordovician extinctions. *Proceedings of the National Academy of Sciences*, **116**, 7207–7213.

Rasmussen, J. A. 1991. Conodont stratigraphy of the Lower Ordovician Huk Formation at Slemmestad, southern Norway. *Norsk Geologisk Tidsskrift*, **71**, 265–288.

Rasmussen, J. A. & Stouge, S. 1995. Late Arenig–early Llanvirn conodont biofacies across the Iapetus Ocean. In *Ordovician Odyssey: Short Papers for the Seventh International Symposium on the Ordovician System* (Cooper, J. D., Droser, M. L. & Finney, S. C., eds), *Pacific Section, Society for Sedimentary Geology (SEPM)*, **77**, 443–447.

Rasmussen, J. A. & Stouge, S. 2018. Baltoscandian biofacies and their link to Middle Ordovician (Darriwilian) global cooling. *Palaeontology*, **61**, 391–416.

Rasmussen, J. A., Bruton, D. L. & Nakrem, H. A. 2013. Stop 17. Tremadocian to Darriwilian units, Bjørkåsholmen and Djuptrekkodden, Slemmestad. In *The Lower Palaeozoic of Southern Sweden and the Oslo Region, Norway: Field Guide for the 3rd Annual Meeting of the IGCP Project 591* (Calner, M., Ahlberg, P., Lehnert, O. & Erlström, M., eds), *Sveriges Geologiska Undersökning Rapporter och meddelanden*, **133**, 67–72.

Raukas, A. & Teedumäe, A. (eds). 1997. *Geology and Mineral Resources of Estonia*. Estonian Academy Publishers, Tallinn, 436 pp.

Raymond, P. E. 1916. Expedition to the Baltic provinces of Russia and Scandinavia. Part I. The correlation of the Ordovician strata of the Baltic Basin with those of eastern North America. *Bulletin of the Museum of Comparative Zoology*, **56**, 179–286.

Rozhnov, S. 2017. Cyanobacterial origin and morphology of the Volkhov hardgrounds (Dapingian, middle Ordovician) of the St. Petersburg region (Russia). *Bollettino della Società Paleontologica Italiana*, **56**, 153–160.

Rozhnov, S. V. & Kushlina, V. B. 1994. Interpretation of new data on *Bolboporites* Pander, 1830 (Echinodermata; Ordovician). In *Echinoderms Through Time* (Bruno, D., Guille, A., Féral, J.-P. & Roux, M., eds), pp. 179–180. A. A. Balkema, Rotterdam.

Schmidt, F. 1858. Untersuchungen über die silurische Formation von Ehstland, Nord-Livland und Ösel. *Archiv für die Naturkunde Liv', Ehst- und Kurlands, Serie 1*, **2**, 1–248.

Schmidt, F. 1881. Revision der ostbaltischen silurischen Trilobiten nebst geognostischer Übersicht des ostbaltischen Silurgebiets. Abtheilung 1: Phacopiden, Cheiruriden und Encrinuriden. *Mémoires de l'Académie Impériale des Sciences de St. Pétersbourg*, **30**, 1–237.

Schmidt, F. 1882. On the Silurian (and Cambrian) strata of the Baltic provinces of Russia, as compared with those of Scandinavia and the British Isles. *Quarterly Journal for the Geological Society*, **38**, 514–536.

Schmitz, B. & Häggström, T. 2006. Extraterrestrial chromite in Middle Ordovician marine limestone at Kinnekulle, southern Sweden – traces of a major asteroid breakup event. *Meteoritics and Planetary Science*, **41**, 455–466.

Schmitz, B., Häggström, T. & Tassinari, M. 2003. Sediment-dispersed extraterrestrial chromite traces a major asteroid disruption event. *Science*, **300**, 961–964.

Schmitz, B., Harper, D. A. T., Peucker-Ehrenbrink, B., Stouge, S., Alwmark, C., Cronholm, A., Bergström, S. M., Tassinari, M. & Xiaofeng, W. 2008. Asteroid breakup linked to the Great Ordovician Biodiversification Event. *Nature Geoscience*, **1**, 49–53.

Selivanova, V. A. & Kofman, L. R. (eds). 1971. *Geologiya SSSR, T.1. Leningradskaya, Pskovskaya i Novgorodskaya oblasti. Geologicheskoe opisanie* [*Geology of the USSR, Volume I, Leningrad, Pskov and Novgorod Regions, Geological Descriptions*]. Nedra Publishing House, Moscow, 502 pp. [in Russian].

Sepkoski, J. J. Jr. 1981. A factor analytic description of the Phanerozoic marine fossil record. *Paleobiology*, **7**, 36–53.

Sepkoski, J. J. Jr. 1995. The Ordovician radiations: diversification and extinction shown by global genus-level taxonomic data. In *Ordovician Odyssey: Short Papers for the Seventh International Symposium on the Ordovician System* (Cooper, J. D., Droser, M. L. & Finney, S. C., eds), *Pacific Section, Society for Sedimentary Geology (SEPM)*, **77**, 393–396.

Sergeyeva, S. P. 1962. Stratigraphic dispersion of conodonts in the Lower Ordovician of the Leningrad province. *Doklady Akademii Nauk SSSR*, **146**, 1393–1395.

Sibley, D. F. & Gregg, J. M. 1987. Classification of dolomite rock textures. *Journal of Sedimentary Petrology*, **57**, 967–975.

Stigall, A. L., Edwards, C. T., Freeman, R. L. & Rasmussen, C. M. Ø. 2019. Coordinated biotic and abiotic change during the Great Ordovician Biodiversification Event: Darriwilian assembly of early Paleozoic building blocks. *Palaeogeography, Palaeoclimatology, Palaeoecology*, **530**, 249–270.

Stouge, S. & Bagnoli, G. 1990. Lower Ordovician (Volkhovian–Kundan) conodonts from Hagudden, northern Öland, Sweden. *Palaeontographica Italica*, **77**, 1–54.

Stouge, S. & Nielsen, A. T. 2003. An integrated biostratigraphical analysis of the Volkhov–Kunda (Lower

Ordovician) succession at Fågelsång, Scania, Sweden. *Bulletin of the Geological Society of Denmark*, **50**, 75–94.

Stouge, S., Bagnoli, G. & Rasmussen, J. A. 2019. Late Cambrian (Furongian) to mid-Ordovician euconodont events on Baltica: invasions and immigrations. *Palaeogeography, Palaeoclimatology, Palaeoecology*, https://doi.org/10.1016/j.palaeo.2019.04.007.

Sturesson, U. 2003. Lower Palaeozoic iron oolites and volcanism from a Baltoscandian perspective. *Sedimentary Geology*, **159**, 241–256.

Sturesson, U., Dronov, A. & Saadre, T. 1999. Lower Ordovician iron ooids and associated oolitic clays in Russia and Estonia: a clue to the origin of iron oolites? *Sedimentary Geology*, **123**, 63–80.

Tabor, N. J., Myers, T. S. & Michel, L. A. 2017. Sedimentologist's guide for recognition, description, and classification of paleosols. In *Terrestrial Depositional Systems: Deciphering Complexities Through Multiple Stratigraphic Methods* (Zeigler, K. E. & Parker, W. G., eds), pp. 165–208. Elsevier, Amsterdam.

Teedumäe, A., Shogenova, A. & Kallaste, T. 2006. Dolomitization and sedimentary cyclicity of the Ordovician, Silurian, and Devonian rocks in South Estonia. *Proceedings of the Estonian Academy of Sciences, Geology*, **55**, 67–87.

Tjernvik, T. E. & Johansson, J. V. 1980. Description of the upper portion of the drill-core from Finngrundet in the South Bothnian Bay. *Bulletin of the Geological Institutions of the University of Uppsala, N.S.*, **8**, 73–204.

Tolmacheva, T. Yu., Holmer, L. E., Dronov, A. V., Egerquist, E., Fedorov, P. V. & Popov, L. E. 1999. Early Ordovician (Hunneberg–Volkhov) facial and faunal changes in the East Baltic. In *Quo vadis Ordovician? Short Papers of the 8th International Symposium on the Ordovician System* (Kraft, P. & Fatka, O., eds), *Acta Universitatis Carolinae – Geologica*, **43**, 467–470.

Tolmacheva, T., Egerquist, E., Meidla, T. & Holmer, L. 2001. Spatial variations in faunal composition, Middle Ordovician, Volkhov Stage, East Baltic. *GFF*, **123**, 65–72.

Tolmacheva, T., Egerquist, E., Meidla, T., Tinn, O. & Holmer, L. 2003. Faunal composition and dynamics in unconsolidated sediments: a case study from the Middle Ordovician of the East Baltic. *Geological Magazine*, **140**, 31–44.

Toom, U., Vinn, O. & Hints, O. 2019. Ordovician and Silurian ichnofossils from carbonate facies in Estonia: a collection-based review. *Palaeoworld*, **28**, 123–144.

Torsvik, T. H. & Cocks, L. R. M. 2017. *Earth History and Palaeogeography*. Cambridge University Press, Cambridge, 317 pp.

Trubovitz, S. & Stigall, A. L. 2016. Synchronous diversification of Laurentian and Baltic rhynchonelliform brachiopods: implications for regional versus global triggers of the Great Ordovician Biodiversification Event. *Geology*, **44**, 743–746.

van der Plas, L. & Tobi, A. C. 1965. A chart for judging the reliability of point counting results. *American Journal of Science*, **263**, 87–90.

Viira, V. 2011. Lower and Middle Ordovician conodonts from the subsurface of SE Estonia and adjacent Russia. *Estonian Journal of Earth Sciences*, **60**, 1–21.

Viira, V., Löfgren, A., Mägi, S. & Wickström, J. 2001. An Early to Middle Ordovician succession of conodont faunas at Mäekalda, northern Estonia. *Geological Magazine*, **138**, 699–718.

Villumsen, J., Nielsen, A. T. & Stouge, S. 2001 The trilobite and conodont biostratigraphy of the upper Volkhov–lower Kunda deposits at Hällekis Quarry, Västergötland, Sweden. In *WOGOGOB-2001 Abstracts* (Harper, D. A. T. & Stouge, S., eds), pp. 30–31. Copenhagen University, Copenhagen.

Webby, B. D., Paris, F., Droser, M. L. & Percival, I. G. (eds). 2004. *The Great Ordovician Biodiversification Event*. Columbia University Press, New York, 484 pp.

Westphal, H., Munnecke, A., Böhm, F. & Bornholdt, S. 2008. Limestone-marl alternations in epeiric sea settings – witnesses of environmental changes, or of rhythmic diagenesis? In *Dynamics of Epeiric Seas* (Pratt, B. R. & Holmden, C., eds), *Geological Association of Canada Special Paper*, **48**, 389–406.

Westphal, H., Hilgen, F. & Munnecke, A. 2010. An assessment of the suitability of individual rhythmic carbonate successions for astrochronological application. *Earth-Science Reviews*, **99**, 19–30.

Wu, R., Stouge, S. & Wang, Z. 2012. Conodontophorid biodiversification during the Ordovician in South China. *Lethaia*, **45**, 432–442.

Wu, R.-C., Calner, M., Lehnert, O., Lindskog, A. & Joachimski, M. 2018. Conodont biostratigraphy and carbon isotope stratigraphy of the Middle Ordovician (Darriwilian) Komstad Limestone, southern Sweden. *GFF*, **140**, 44–54.

Young, T. P. 1992. Ooidal ironstones from Ordovician Gondwana: a review. *Palaeogeography, Palaeoclimatology, Palaeoecology*, **99**, 321–347.

Zaitsev, A. V. & Kosorukov, V. L. 2008. Condensed Lower–Middle Ordovician carbonate deposits in the northwest of the Russian Platform: characteristics of the clay component. *Moscow University Geology Bulletin*, **63**, 38–48.

Zaitsev, A. V. & Pokrovsky, B. G. 2014. Carbon and oxygen isotope compositions of Lower–Middle Ordovician carbonate rocks in the northwestern Russian Platform. *Lithology and Mineral Resources*, **49**, 272–279.

Zhang, J. 1997. The lower Ordovician conodont *Eoplacognathus crassus* Chen & Zhang, 1993. *GFF*, **119**, 61–65.

Zhang, J. 1998a. Conodonts from the Guniutan Formation (Llanvirnian) in Hubei and Hunan provinces, south-central China. *Stockholm Contribution in Geology*, **46**, 1–161.

Zhang, J. 1998b. Middle Ordovician conodonts from the Atlantic faunal region and the evolution of key conodont genera. *Meddelanden från Stockholms universitets institution för geologi och geokemi*, **298**, 1–27.

Kesk-Ordoviitsiumi karbonaatsete faatsieste areng, konodontide biostratigraafia ja fauna mitmekesisuse mustrid Lõnna jõe läbilõikes Loode-Venemaal

Anders Lindskog, Mats E. Eriksson, Jan A. Rasmussen, Andrei Dronov ja Christian M. Ø. Rasmussen

Ordoviitsiumi ajastu on tuntud kui dünaamiline periood Maa ajaloos. Põhjalikud krono-, bio- ja kemostratigraafilised uuringud on loonud detailse ajalise taustsüsteemi, kuid mitmed kohalikud läbilõiked üle maailma alles ootavad analüüsimist. Käesolevas artiklis on esitatud Loode-Venemaa ühe tugiläbilõike, Lõnna jõe paljandi kõrglahutusega andmestiku analüüsi tulemused. Sellel läbilõikel oli juba varasemalt oluline tähtsus Ordoviitsiumi biomitmekesistumise kronoloogia dokumenteerimisel. Nüüd lisati sellele paleokeskkonna makro- ja mikroskoopiline iseloomustus, mis haakub globaalse andmestikuga. Töö tulemused täiendavad arusaama Balti paleobasseini ehitusest ja arengust. Selgus, et mikrofaatsiesed varieeruvad koos kivimite makroskoopiliste tunnustega: puhtamad lubjakivid on jämedama struktuuriga ja savikamad intervallid peenemateralised. Koos kivimi terasuurusega varieerub rütmiliselt ka detriidi taksonoomiline koostis. Kivimid on osaliselt dolomiidistunud, dolomiitsus suureneb läbilõike ülemiste kihtide suunas. Regionaalne võrdlus näitas, et mikro- ja makrolitoloogilised tunnused on seotud meretaseme muutustega. Kõrgresolutsiooniga konodontide biostratigraafia kinnitas varasemaid korrelatsioone, mis baseerusid trilobiitide biotsoonidel ja litoloogial, võimaldades täpsemat rööbistamist läbilõigetega mujal maailmas.